DEFECT STRUCTURES IN COLLOIDAL AND CHIRAL NEMATICS: FROM BRAIDS TO KNOTS

S. ŽUMER
University of Ljubljana & Jozef Stefan Institute & CO NAMASTE, Ljubljana, Slovenia

Support of Slovenian Research Agency and EU ITN network HIERARCHY is acknowledged

COWORKERS & COLLABORATORS

Coworkers (simulations& theory): S. ČOPAR, J. FUKUDA, T. PORENTA, M. RAVNIK




Collaborators (experiments): I.MUŠEVIČ, M.ŠKARABOT, U.TKALEC, V.S.R. JAMPANI

Helpful discussions: R. KAMIEN, O. LAVRENTOVICH, T. LUBENSKY

OUTLINE

- motivation
- nematic mediated inter-particle interaction
- phenomenological description & modeling
- colloidal particles entangled by disclinations
- geometry and topology of disclination loops
- self-linking number
- restructuring and stability of braids
- knots and links; classification
- conclusions

MOTIVATION

- Basic interest in topology of complex structures,
- Richness of nematic braids: knots & links,
- Knotting of DNA (Miluzzi et al.) and light (Dennis et al.),
- Stable 1D, 2D, and 3D colloidal nematic structures,
- Assembling of photonic structures & metamaterials,
- Broad temperature range blue phases (Coles et al.)
- Discovery of skyrmions in chiral magnets (Rossler et al.)

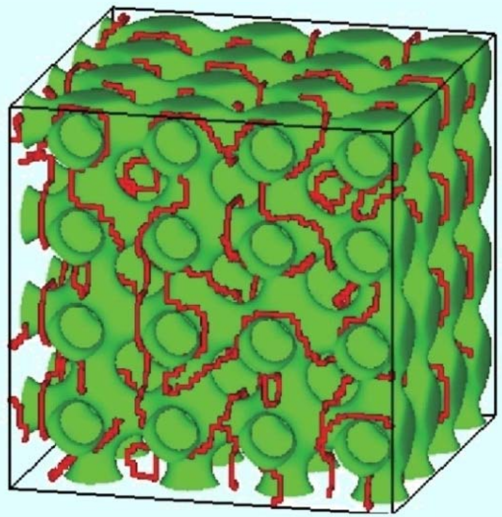

Araki et al. 2011

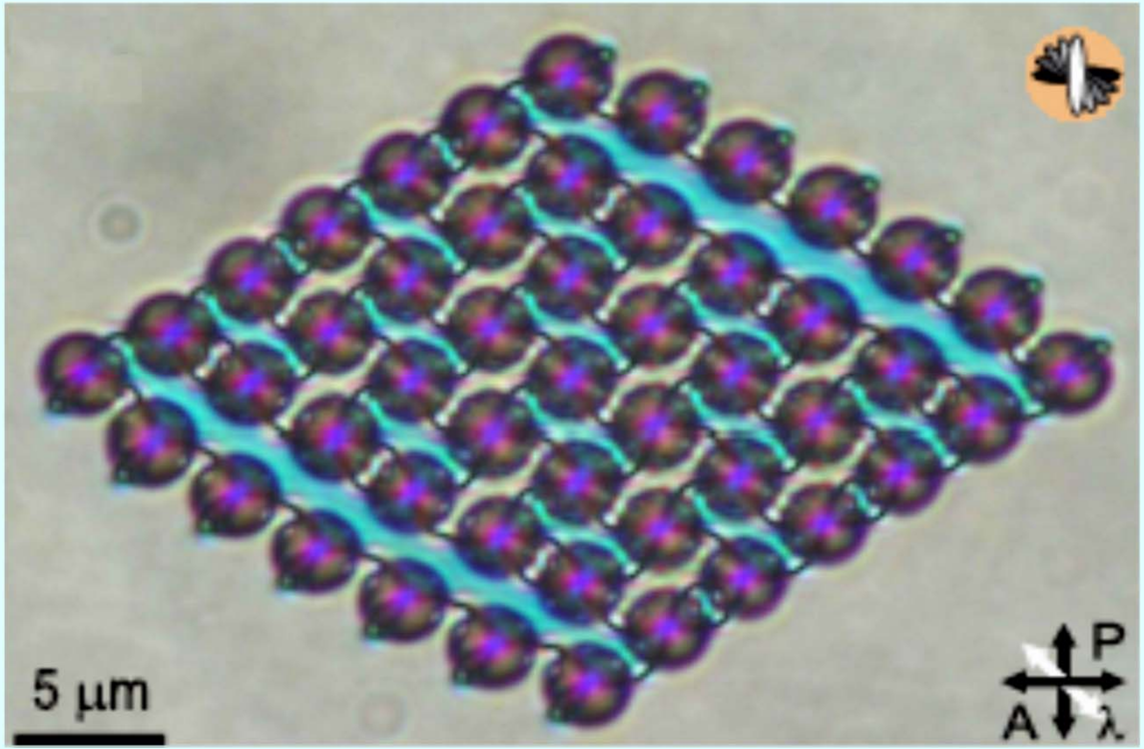

Tkalec et al. 2011

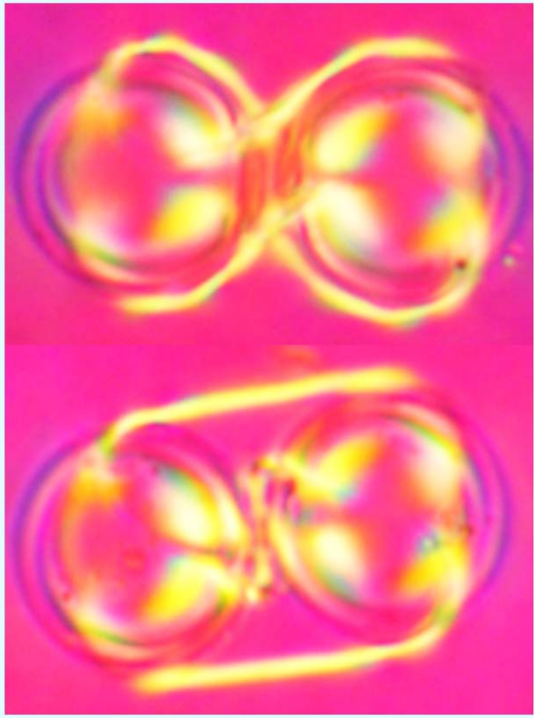

Jampani et al. 2011

NEMATIC ORDER

Scalar nematic order parameter

nematic phase

$$S = < P_2(\cos\vartheta) >$$

Director **n** to –**n** symmetry

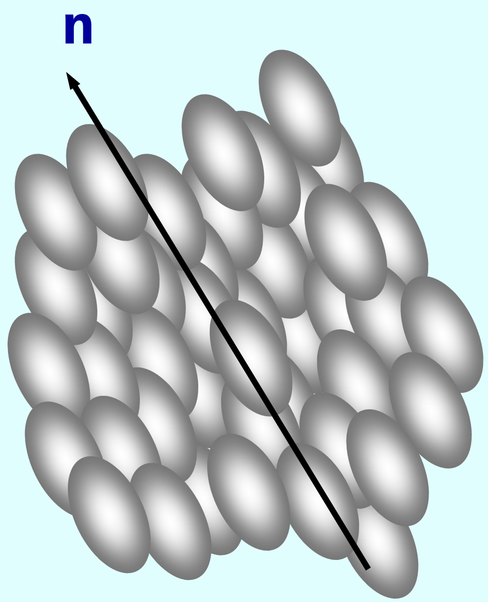

Fluctuations

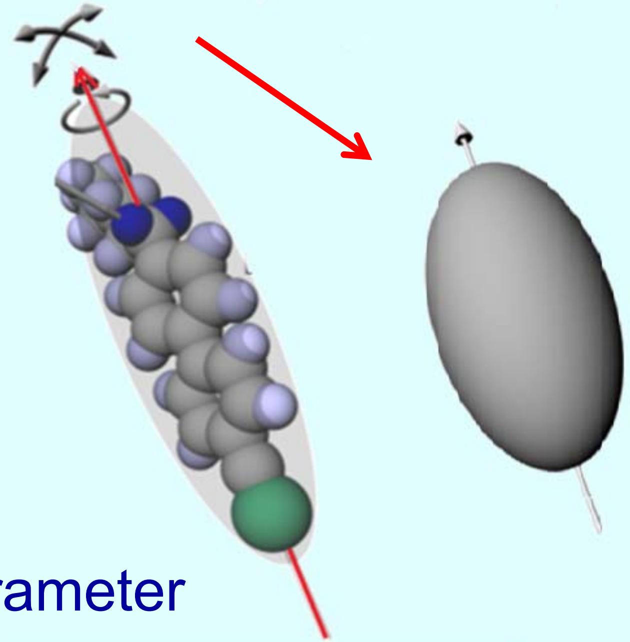

Tensorial order parameter

$$Q_{ij} = \frac{S}{2}(3n_i n_j - \delta_{ij}) + \frac{P}{2}(e_i^{(1)} e_j^{(1)} - e_i^{(2)} e_j^{(2)})$$

Eigen frame: $\boldsymbol{n}$, $\boldsymbol{e}^{(1)}$, $\boldsymbol{e}^{(2)}$, eigen values:

$$\underline{Q} = \begin{bmatrix} -(S+P)/2 & 0 & 0 \\ 0 & -(S-P)/2 & 0 \\ 0 & 0 & S \end{bmatrix}$$

DEFORMED NEMATIC: ELASTIC ENERGY

Basic deformations (Frank elasticity)

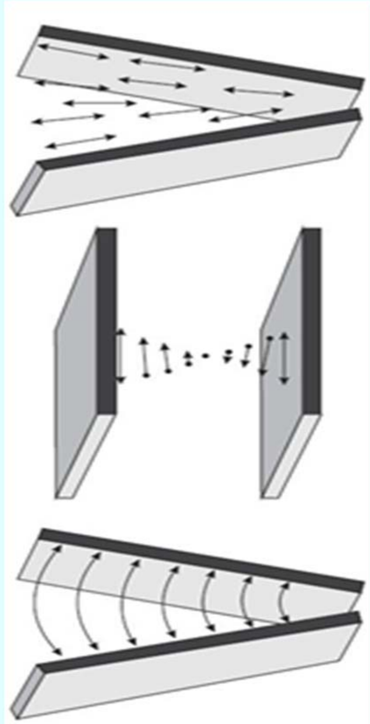

Splay $\nabla \cdot \mathbf{n}$

Twist $\mathbf{n} \cdot (\nabla \times \mathbf{n})$

Bend $\mathbf{n} \times (\nabla \times \mathbf{n})$

Surface anchoring $\mathbf{n} \cdot \nu$

Order variation, Surface elasticity, Flexoelectricity, External fields….

DEFECTS

- discontinues director fields & variation in nematic order (2D&3D objects)
- defects are formed after fast cooling, or by other external perturbations,
- topological picture (symmetry of the order parameter - director field, equivalences, and conservation laws):

- point defects:

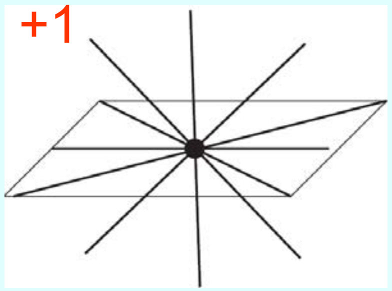

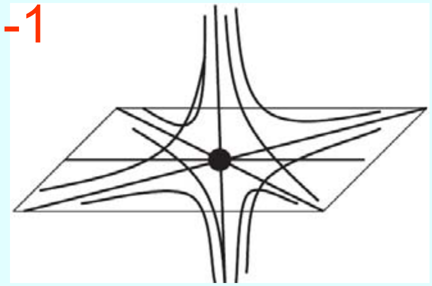

  - topological charge

$$q = \frac{1}{2} \oint dS_i \epsilon_{ijk} \vec{n} \cdot (\partial_j \vec{n} \times \partial_k \vec{n})$$

- line defects (disclinations) :

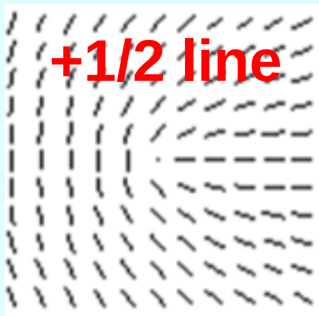

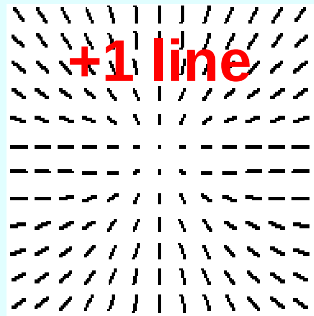

  - winding number,
  - topological charge of a loop

- core structure:

biaxiality & decrease of order (tensorial fields)

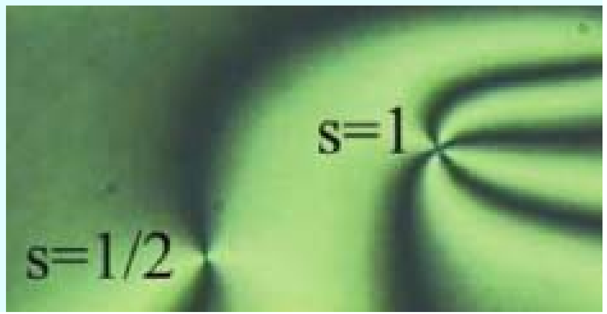

CONFINEMENT

Planar (thin layers)

Cylindrical

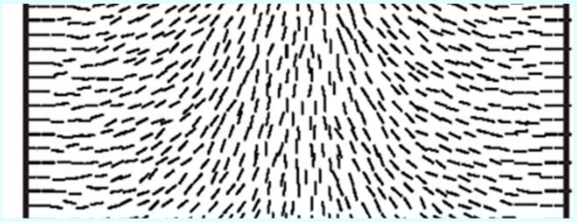

Spherical

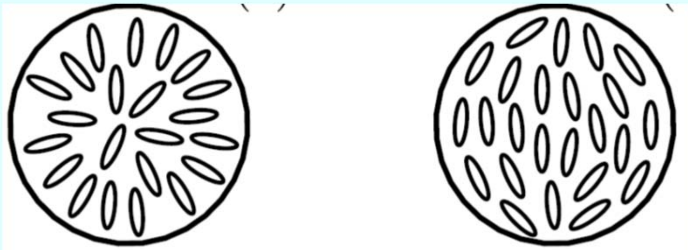

Colloidal particles => nematic colloidal dispersion

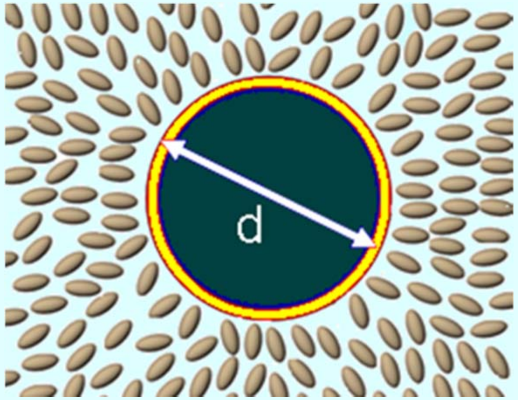

Confinement scale & Extrapolation length

elastic constant / anchoring strength

SPONTANEOUS DEFORMATION: CHIRAL NEMATIC

How LC molecules are arranged in chiral nematic phases?

achiral molecules — chiral molecules spontaneous

nematic phase — weak chirality — cholesteric phase

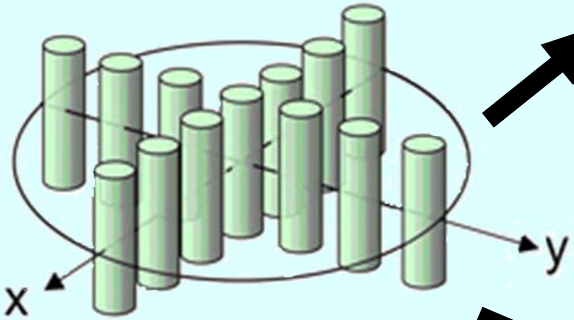

nematic uniform alignment

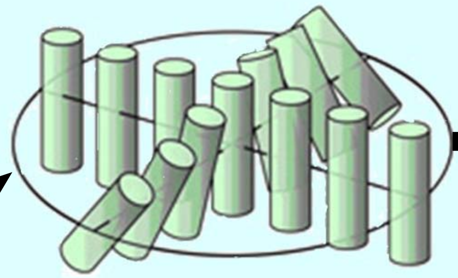

single twist

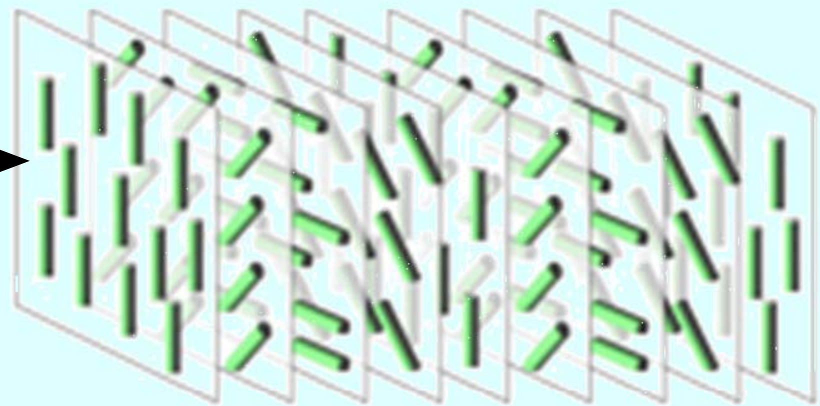

pitch

strong chirality

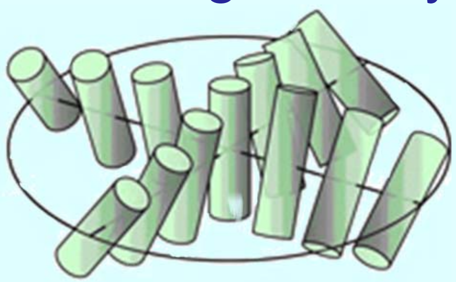

double twist

blue phases

http://kikuchi-lab.cm.kyushu-u.ac.jp/kikuchilab/bluephase.html

TENSORIAL NEMATIC FREE ENERGY

Landau - de Gennes free energy based on the tensorial nematic order parameter *Q*

$$Q_{ij} = \frac{S}{2}(3n_i n_j - \delta_{ij}) + \frac{P}{2}(e_i^{(1)} e_j^{(1)} - e_i^{(2)} e_j^{(2)})$$

includes: the standard phase term, the one constant bulk elastic (gradient) term that has chiral symmetry and a term inducing the nematic anchoring preferred by confining surfaces:

$$\begin{aligned} F \; = \; & \int_{LC} \left(\frac{1}{2} A Q_{ij} Q_{ji} + \frac{1}{3} B Q_{ij} Q_{jk} Q_{ki} + \frac{1}{4} C (Q_{ij} Q_{ji})^2 \right) dV \\ & + \frac{1}{2} L \int_{LC} \left(\frac{\partial Q_{ij}}{\partial x_k} \frac{\partial Q_{ij}}{\partial x_k} + 4 q_0 \epsilon_{ikl} Q_{ij} \frac{\partial Q_{lj}}{\partial x_k} \right) dV \\ & + \frac{1}{2} W \int_{Conf.\ Surf.} (Q_{ij} - Q_{ij}^0)(Q_{ji} - Q_{ji}^0) dS_c \end{aligned}$$

Equilibrium & metastable chiral nematic structures are determined via numerical minimization of F that leads to the solving of the corresponding coupled partial differential equations.

SEARCH FOR STRUCTURES

- Minimization of free energy yields stable and metastable structures.

- Explicit Euler finite difference relaxation on cubic mesh typically covers $10^6 - 10^7$ mesh points. Limit on sample size that includes defects comes from nematic correlation length

$$\xi_N = \sqrt{L/(A + BS + 9/2CS^2)}$$

ξ_N = 5 – 10 nm that requires around 10 nm lattice distance for the finer mesh and 100nm for the low resolution mesh. Usually 10^4 to 10^5 steps are needed.

- Boundary conditions :

  - Conditions on confining surfaces and on surfaces of collodal particles are controlled via corresponding free energy contributions.

  - Open boundary conditions on surfaces where is no confinement.

VISUALIZATION

Visualization of defect using tensor al order parameter:

- Director lines are useful for structures but not enough for defects where order is depressed.
- Surfaces of constant order parameter - S are useful for visualization of the disclination lines with singular cores. Substantial decrease only in the range of few ξ_N

Example: -1/2 disclination:

iso-surface

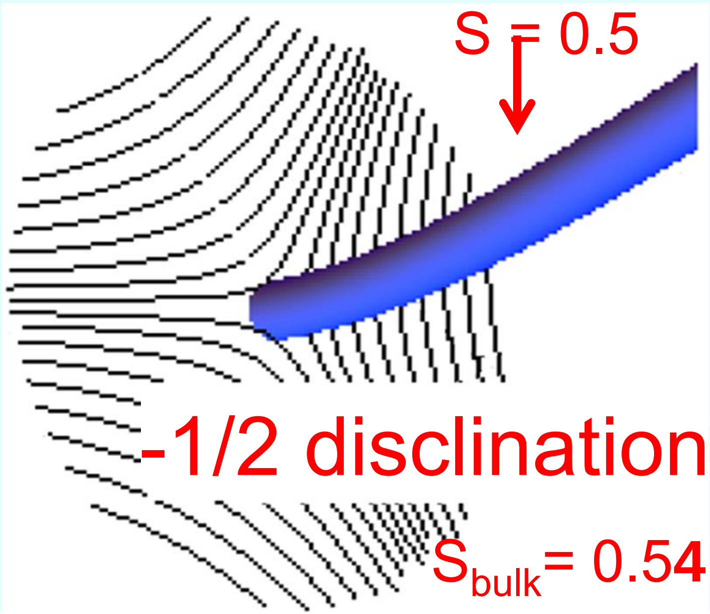

3 fold ribbon

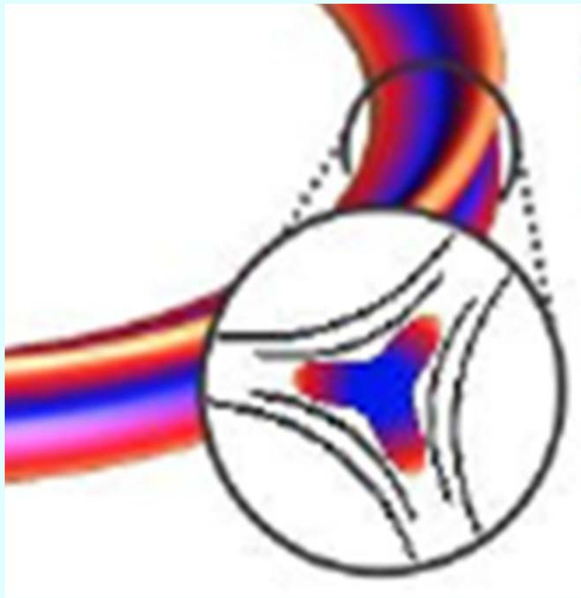

VISUALIZATION

Visualization of defect using derivatives of the tensorial order parameter:

- Surfaces of constant derivatives of order parameter are useful to stress specific deformations of the ordering field.

Example: -1/2 disclination:

splay & bend deformation
blue & yelow

$$S_{SB} = \frac{\partial^2 Q_{ij}}{\partial x_i \partial x_j} \xi_N^2$$

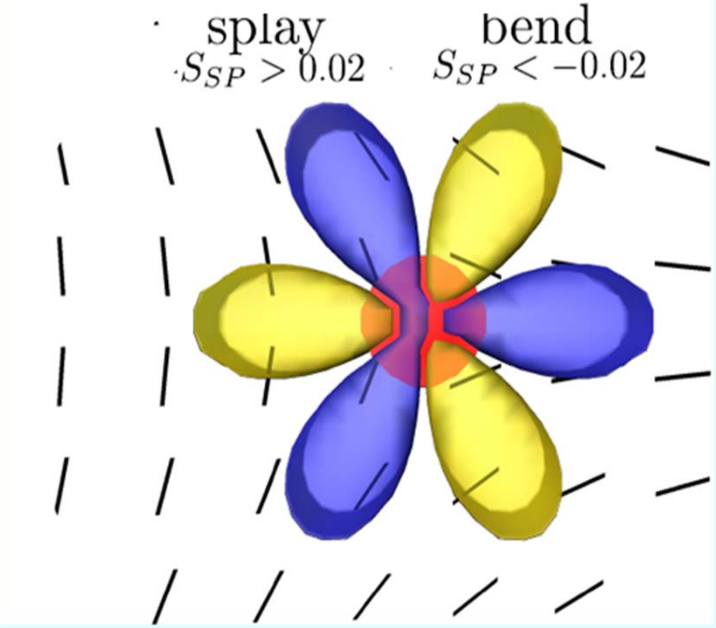

twist deviation from natural values
green & purple

$$S_{TW} = \left(\varepsilon_{ikl} Q_{ij} \frac{\partial Q_{lj}}{\partial x_k} - \frac{9}{4} S^2 q_0\right) \xi_N$$

$= \pm 0.018$

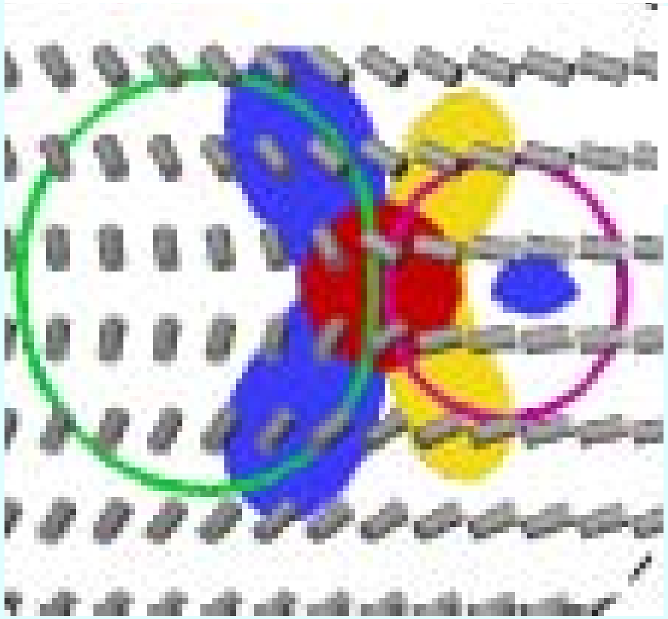

Copar et al.
Soft Matter
2012

HOMEOTROPIC PARTICLES IN NEMATICS

PARTICLES IN A HOMOGENOUS NEMATIC FIELD

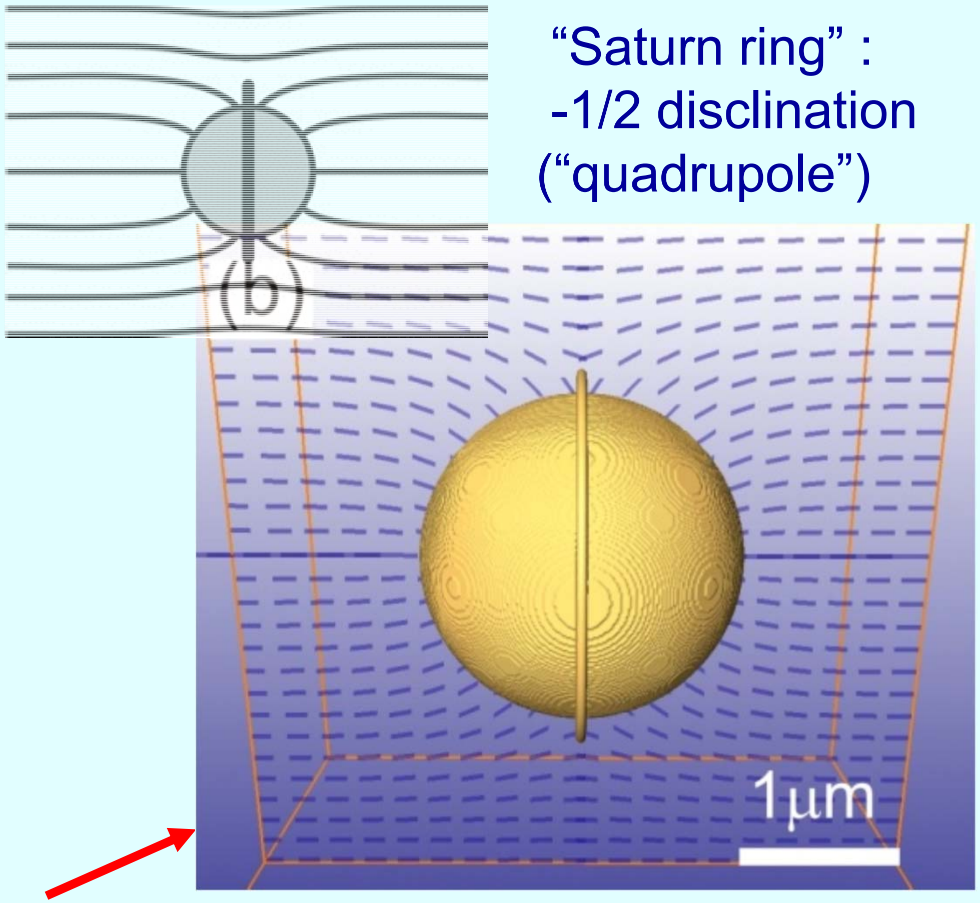

“Saturn ring” :
-1/2 disclination
(“quadrupole”)

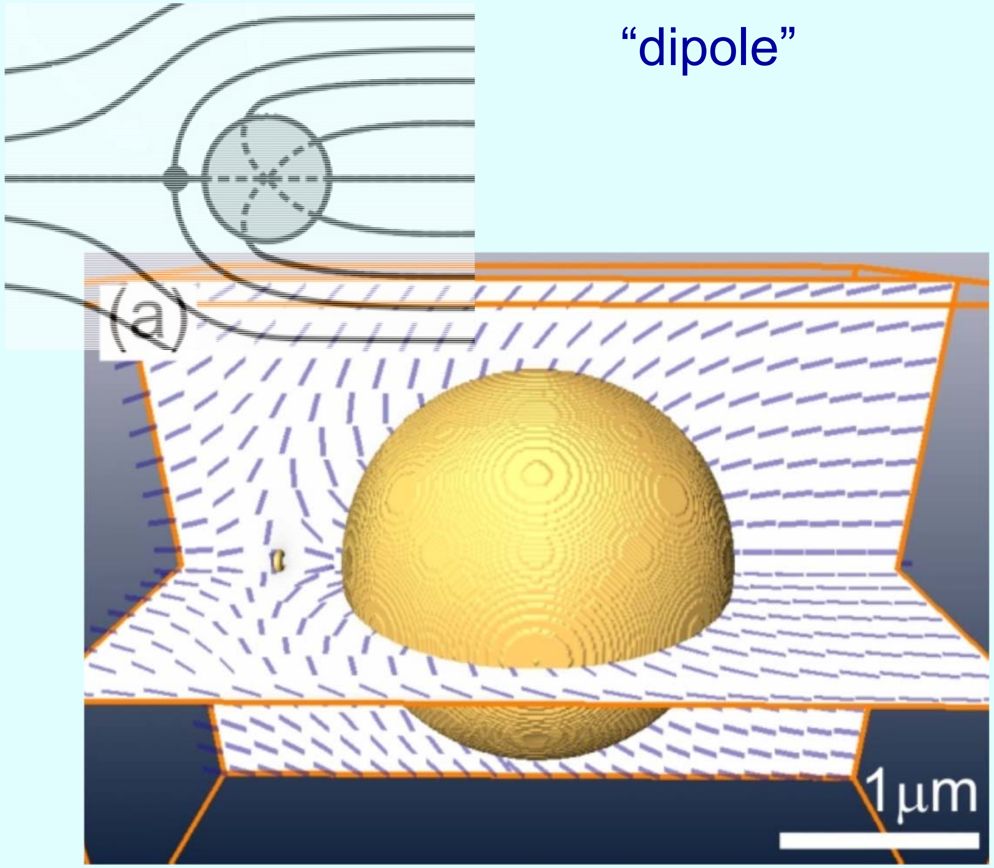

“dipole”

Smaller diameter, weaker anchoring
or stronger confinement

Stark et al., NATO Science Series Kluwer 02

CONFINEMENT OF COLLOIDS TO THIN LAYERS

- Thin layer of a nematic or chiral nematic liquid crystal within a cell that provides two strong unidirectional anchoring directions that are either parallel for planar cells and twist cells with π, 2π... twist and orthogonal for twist cells with $\pi/2$, $3\pi/2$... twist.
- Severe confinement of collodal particles: h ~ d and two !

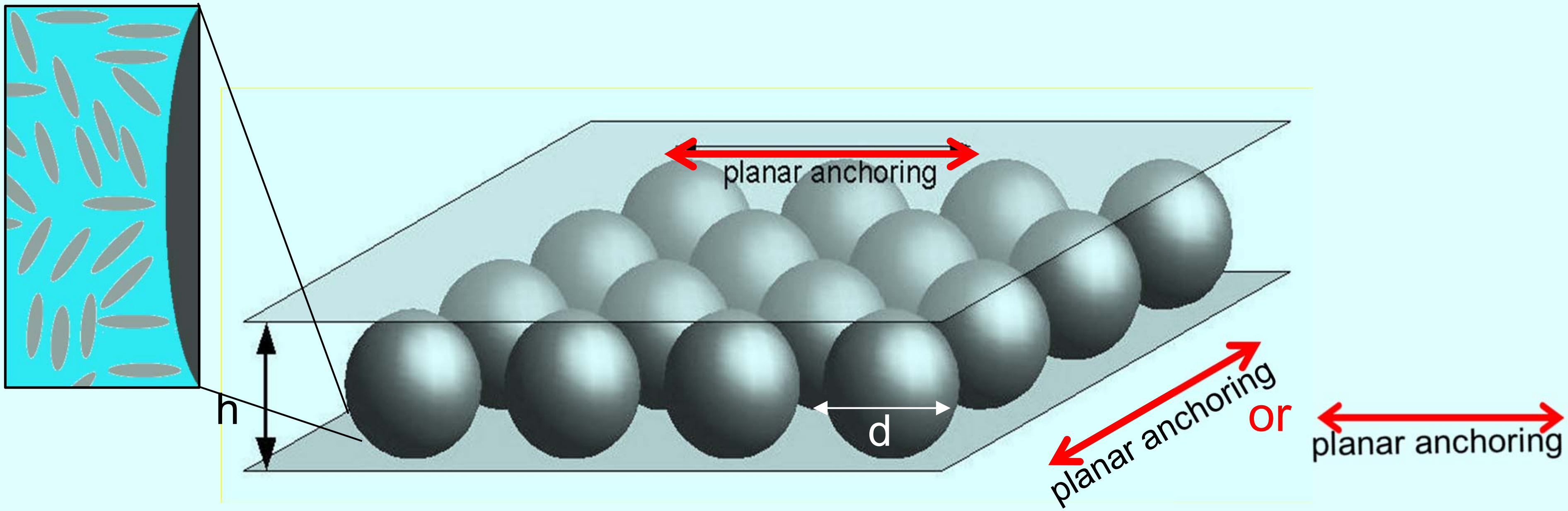

- Particle sizes d: micron range.
- Strong homeotropic anchoring (Wd/L >>1) on particle surfaces is assumed.

EFFECTIVE INTERACTIONS: CLUES TO ASSEMBLING

Nematic mediate effective particle – particle interaction as a result of the minimization of the total free energy – > “thermodynamic” forces. Mechanisms:

- ❑ Sharing of deformed areas associated to the defects & disclinations localized to colloidal particles. Distance dependent: power law & confinement induced screening
  - Dipolar and quadrupolar

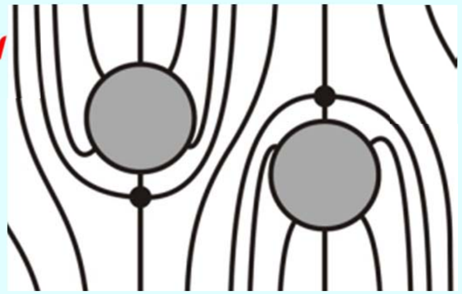

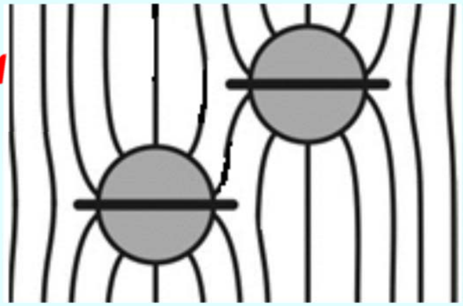

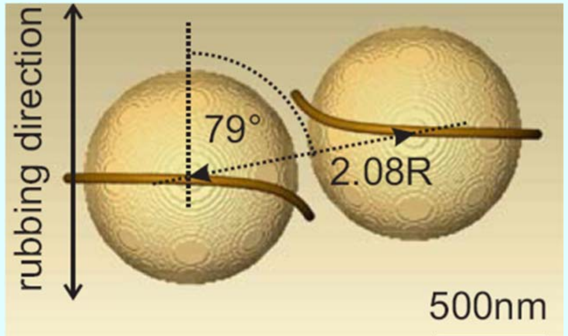

- ❑ Sharing of disclinations: string like interactions (entanglement)

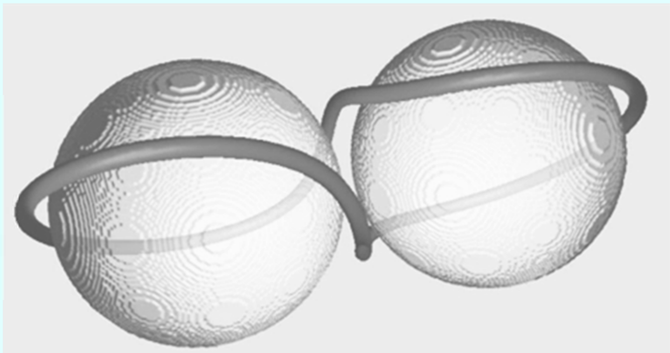

QUENCH AND ENTANGLED PAIR

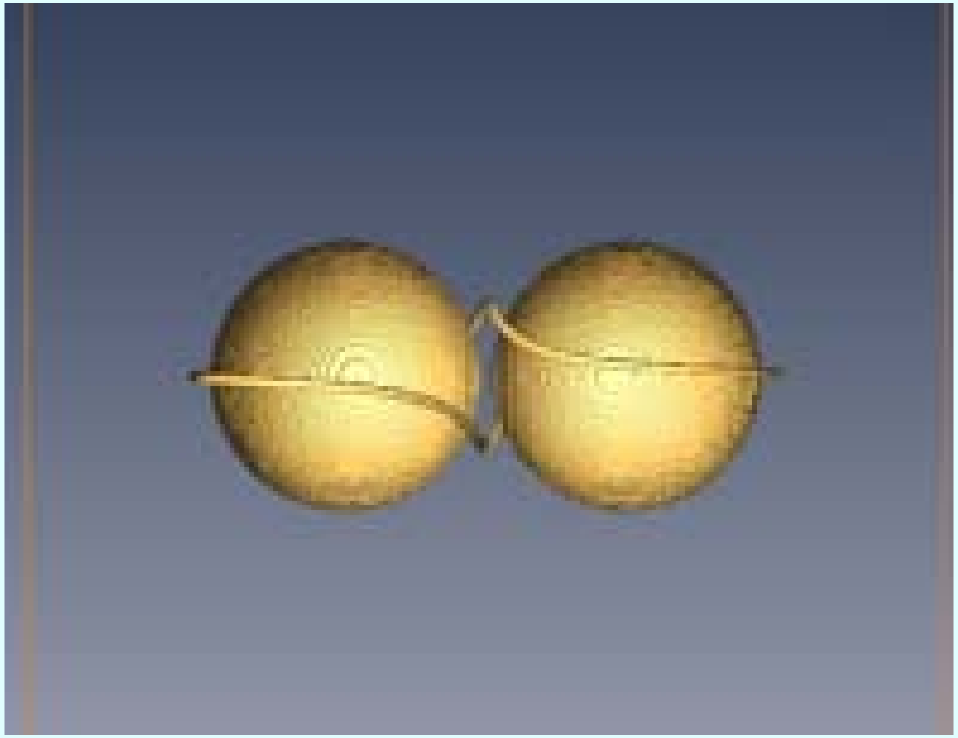

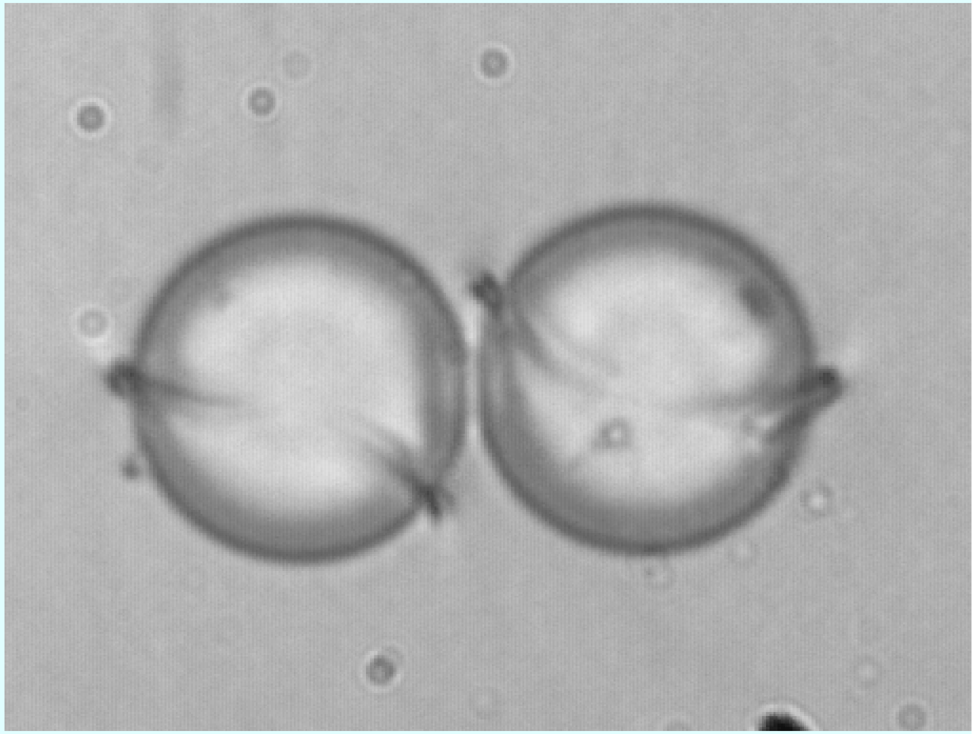

director

M.Ravnik et al., *Phys. Rev. Lett.* (2007)

COLLOIDAL DIMER

IN A HOMOGENOUS NEMATIC FIELD (planar cell)

zero total topological charge

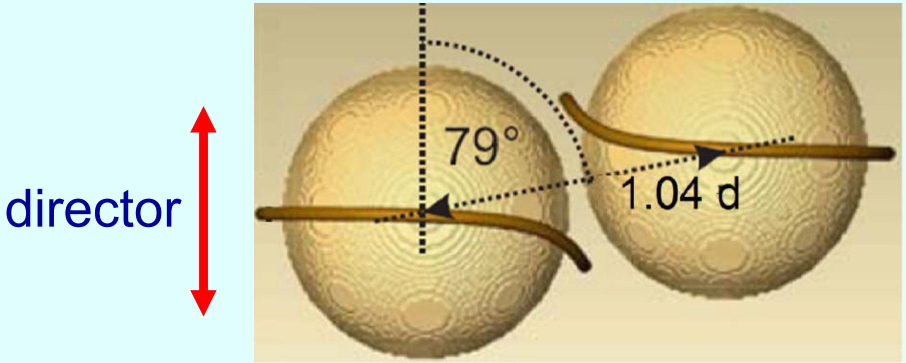

cell thickness: h = 2 μm ,
colloid diameter: d = 1 μm

In homogenous nematic restructuring goes only via local melting & quenching

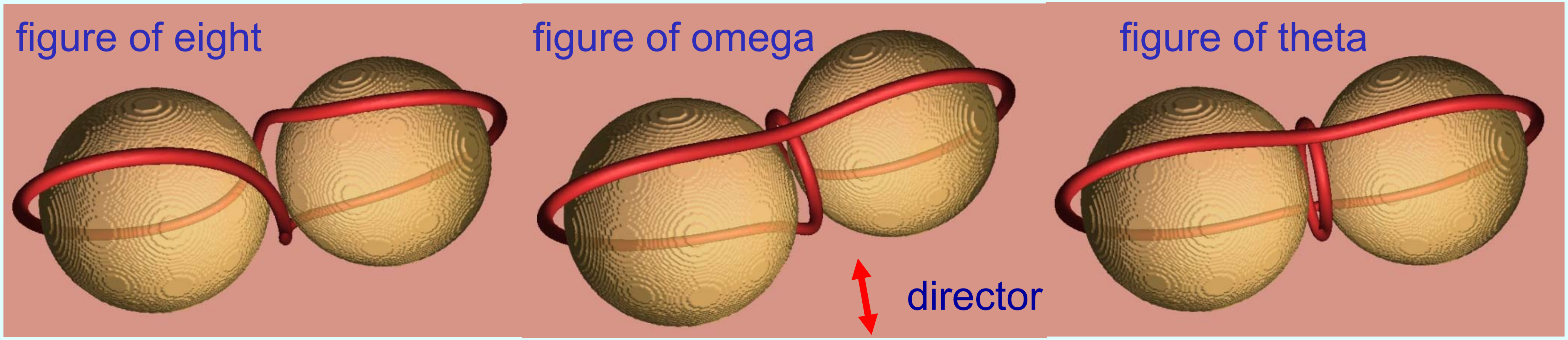

- metastable states with few % higher free energy.
- high energy barrier (several thousand kT) for micron size particles

  ↳ Ravnik et al. PRL2007, Soft Matter 2009

- coupling comparable kT for nano particles

  ↳ Guzman et al. 2003, Araki&Tanaka 2006, Huang et al. 2006

RESTRUCTURING VIA TETRAHEDRON REORIENTATION

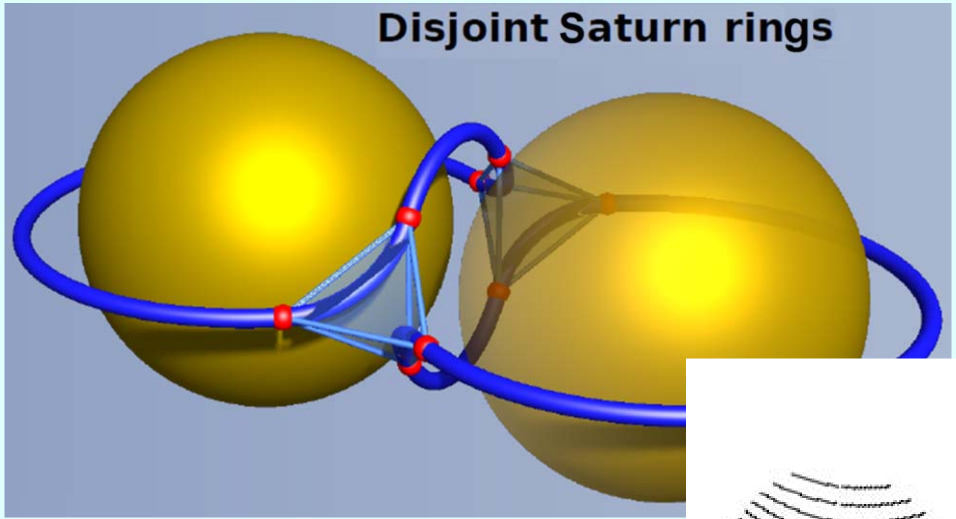

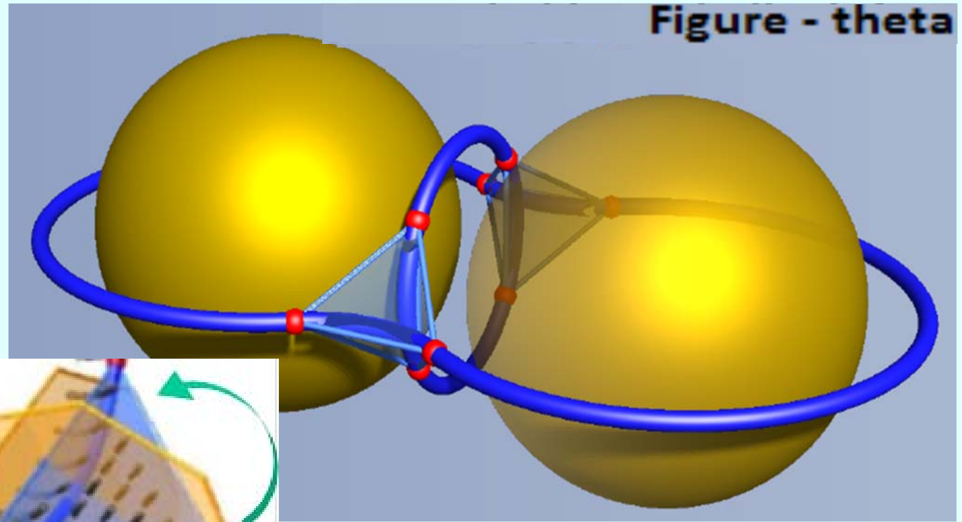

Orthogonal crossing of disclinations in a tetrahedron

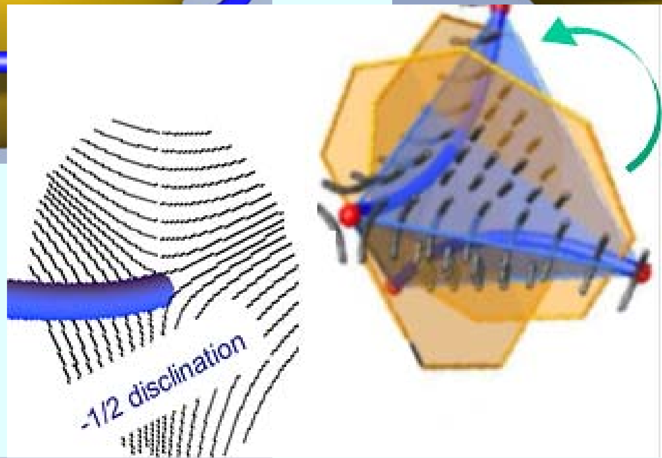

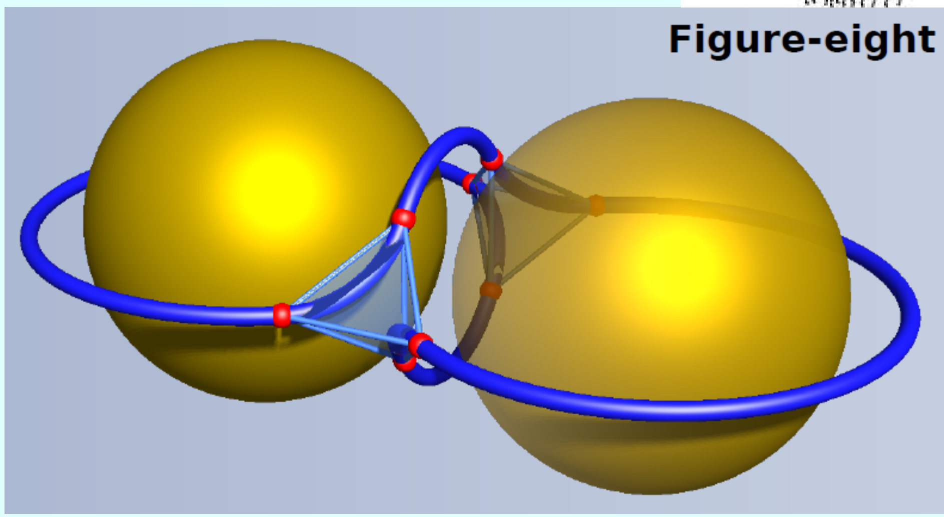

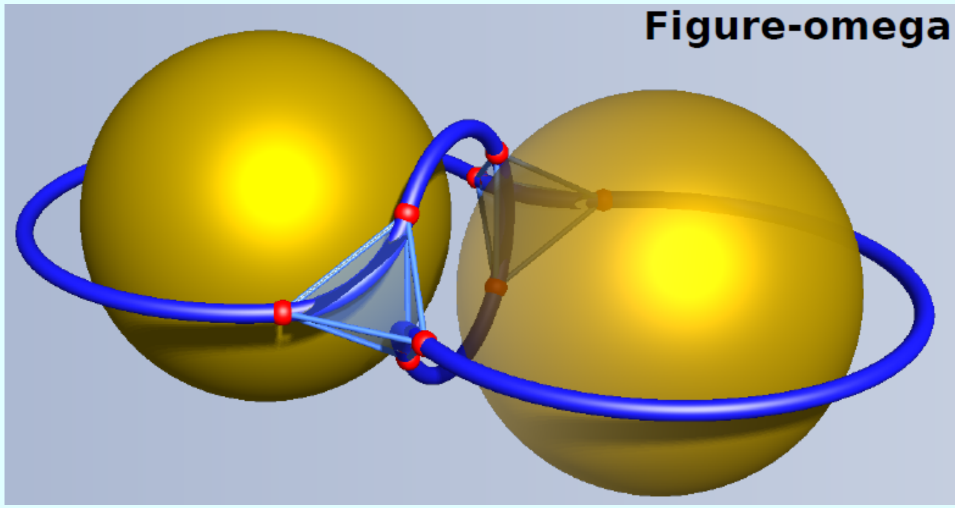

Figure of eight and figure of theta have left and right structures so that 6 different configurations are topologically possible.

Copar & Zumer PRL 2011

RIBBONS forming LOOPS

All disclinations are -1/2 lines ⟶ ribbons with three fold symmetry

geometrical twist & writhe

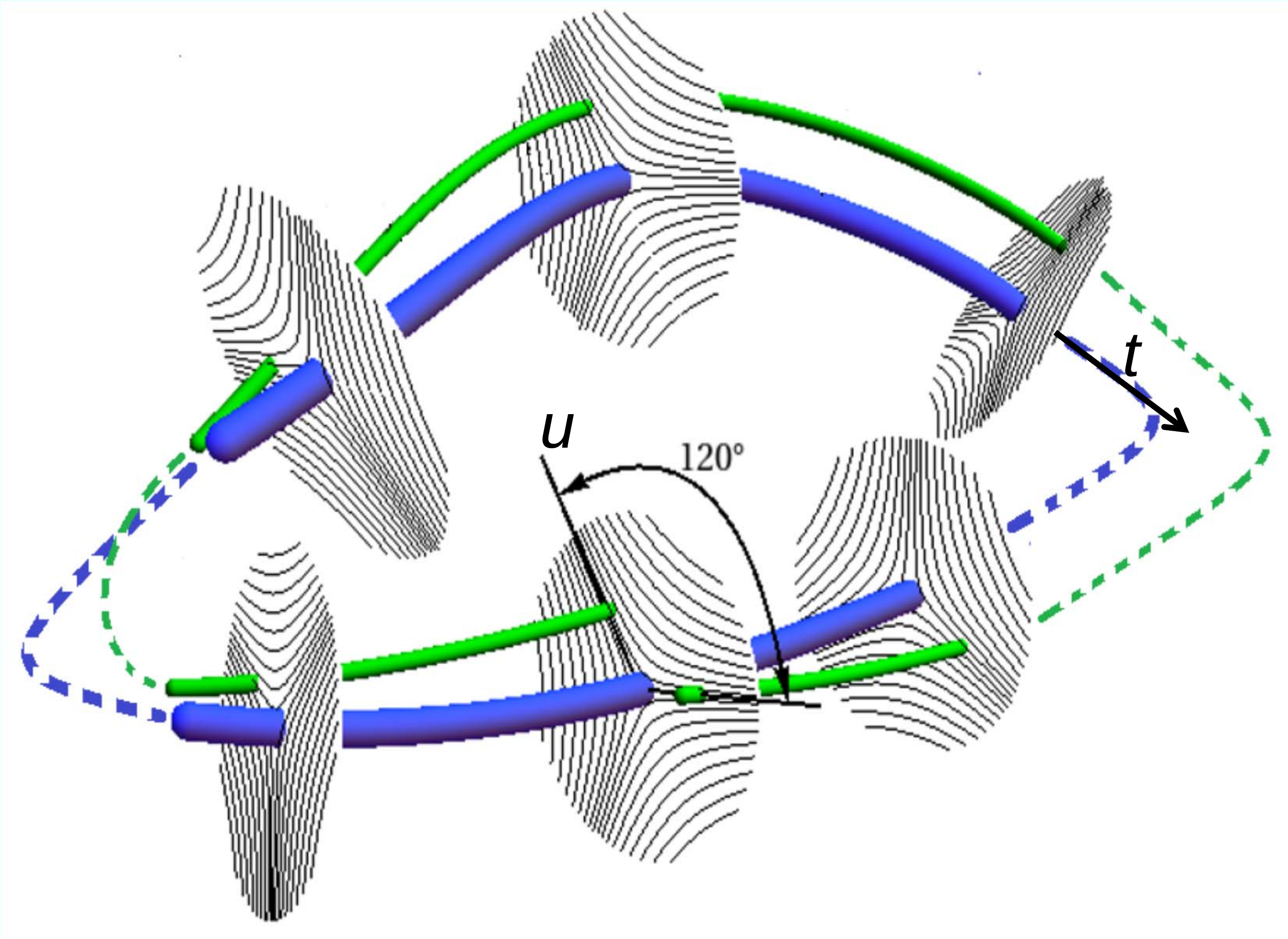

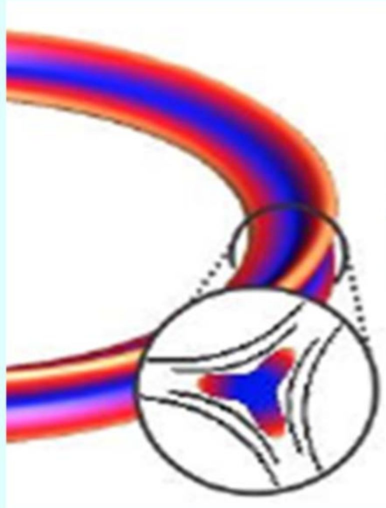

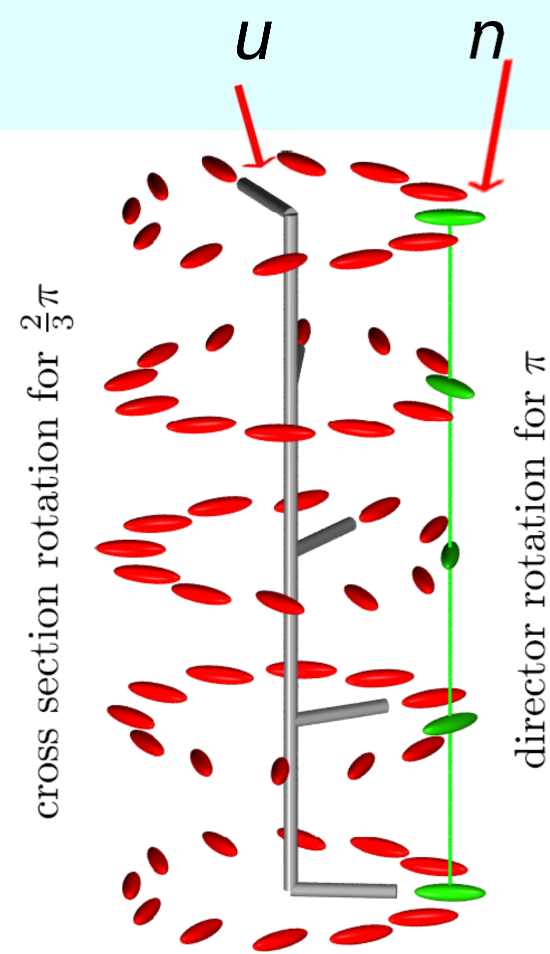

director twist determines twist part of elastic energy

TWIST & WRITHE

Geometrical properties of ribbons

$$Tw = \frac{1}{2\pi}\int \mathbf{t}(s)\cdot(\mathbf{u}(s)\times\partial_s\mathbf{u}(s))\,\mathrm{d}s$$

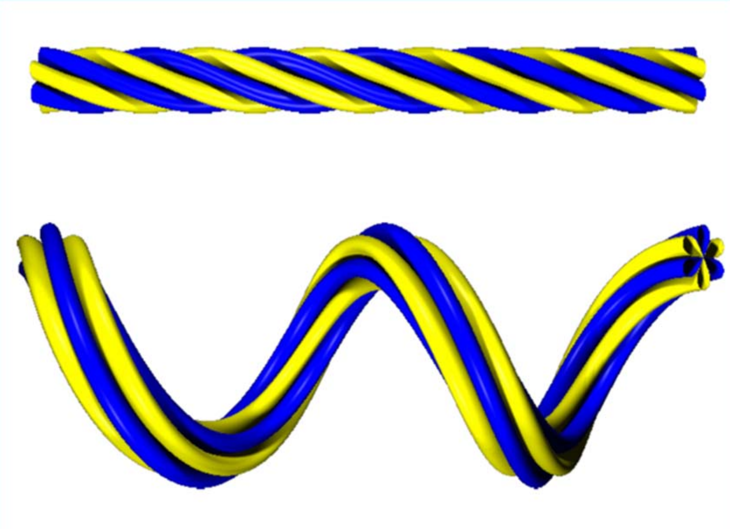

Twist : line integration of local twist along the loop.

Writhe: 2D integral measuring how tangent at different segments of the loop is related. Zero for planar loops.

$$Wr = \frac{1}{4\pi}\iint \mathbf{t}(s)\times\mathbf{t}(s')\cdot\frac{\mathbf{r}(s)-\mathbf{r}(s')}{|\mathbf{r}(s)-\mathbf{r}(s')|^3}\,\mathrm{d}s\,\mathrm{d}s'$$

Copar & Zumer PRL 2011

SELF-LINKING NUMBER, WRITHE & TWIST

Introduction of the topological invariant for disclination loops (ribbons) the self-linking number that is equal to the number of times the ribbon turns around its tangent before closing a loop.

Assumption : transverse profile of the ribbon is preserved!

Calugareanu theorem (1959):

$$Sl = Wr + Tw$$

Where writhe and twist are given by above introduced integrals performed on closed loops.

Examples:

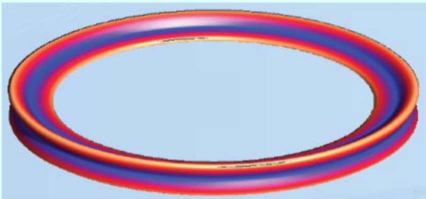

Saturn ring: $Wr = 0$, $Tw = 0$

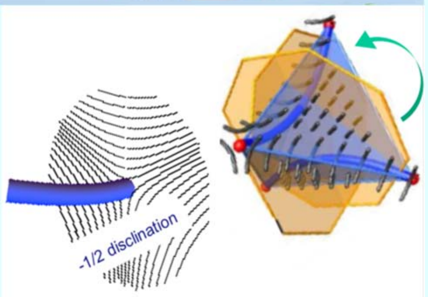

Loops entangling dimers: Tetrahedron restructuring contributes only to the change of writhe as 3-fold symmetry allow only 120^0 reorientations! Therefore we expect that dimer loops has $Tw \cong 0$

Copar & Zumer PRL 2011

CALCULATION OF WRITHE

Following Fuller (1978) writhe is calculated in tangent representation on a unit sphere

$$\mathrm{Wr} = \frac{A}{2\pi} - 1$$

A - surface on a unit sphere in tantrix space encircled by the tangent

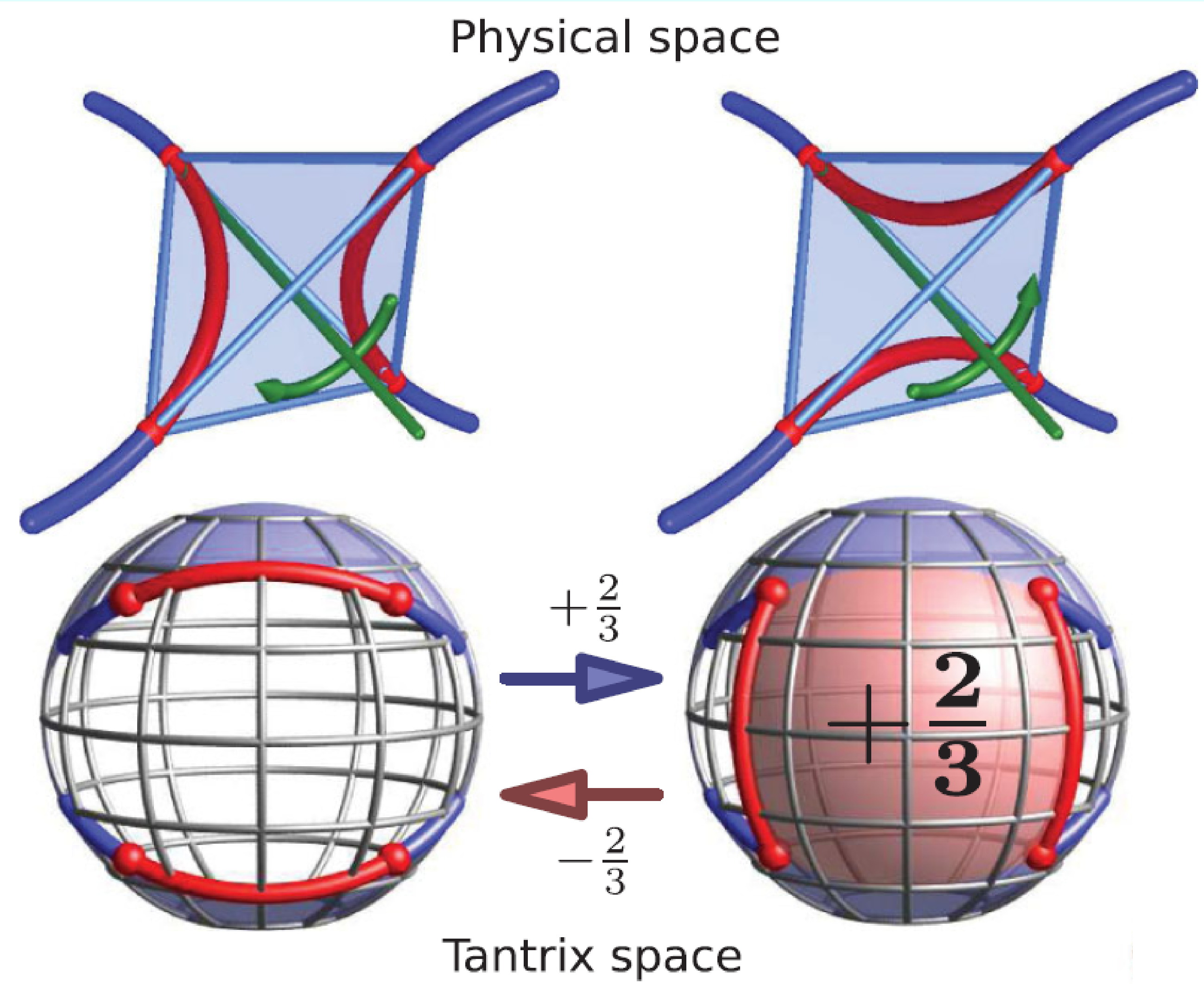

Copar & Zumer
PRL 2011

CLASSIFICATION: NEMATIC COLLOIDAL DIMERS

Assumption: for all our loops $Tw = 0$

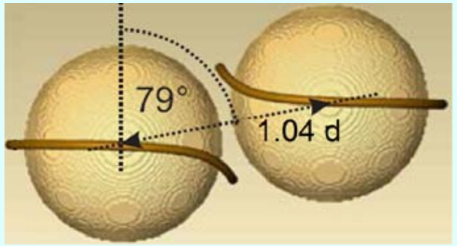

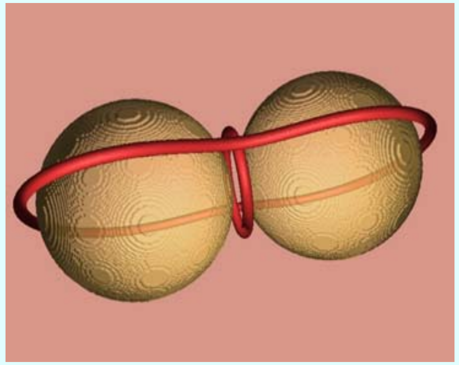

Disjoint Saturns	$Sl = Wr = 0$
Figure of theta	$Sl = Wr = 0$
Figure of eight	$Sl = Wr = \underline{+}\ 2/3$
Figure of omega	$Sl = Wr = \underline{+}\ 2/3$

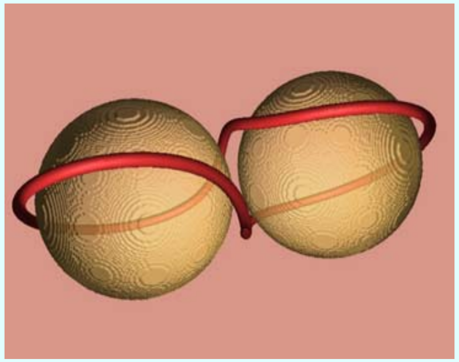

Structures differ in free energy.
Left-right degeneracy is removed in twisted cells.

Copar & Zumer PRL 2011 & supplement

ENTANGLEMENT: STRING LIKE BOND

Disclination provides a long range string like bond. The inter particle force is distance independent as free energy is proportional to the disclination length!

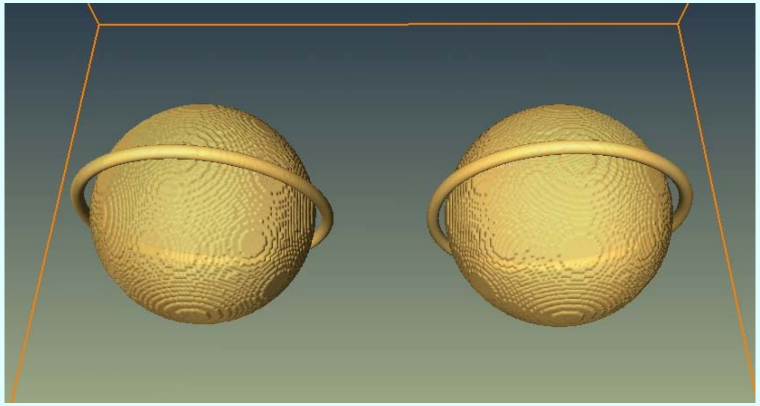

Experiment:
d= 4.7 μm
h= 6 μm

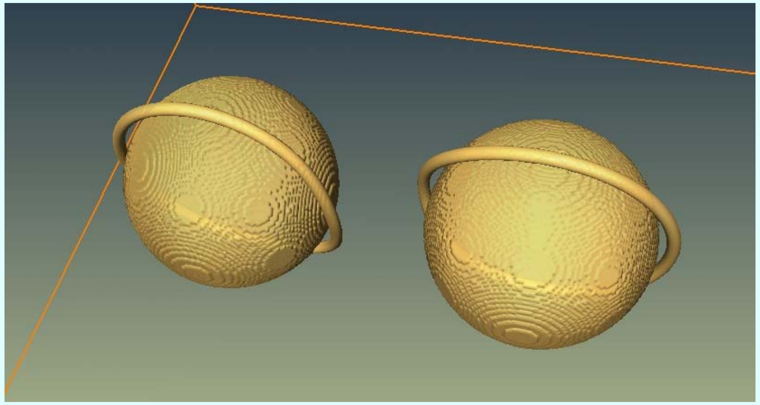

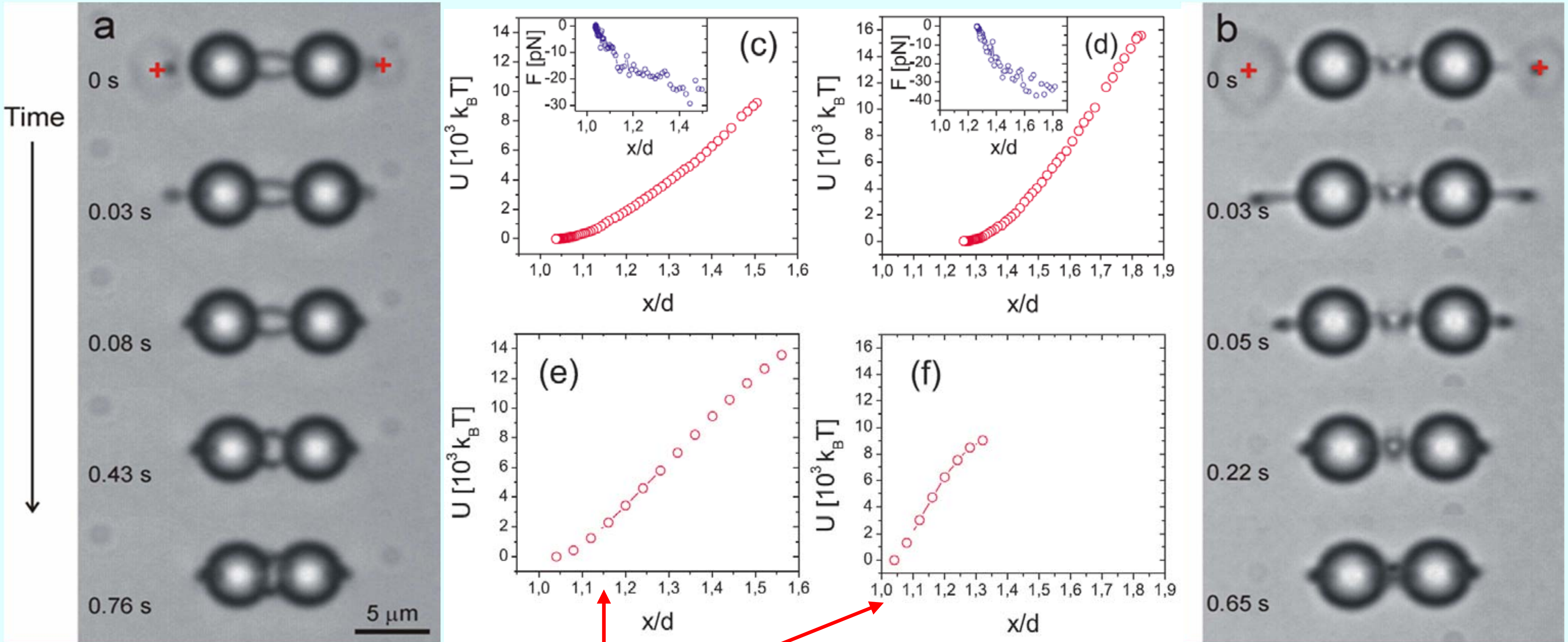

Calculated d=1μm, h=2μm case renormalized to experimental colloid size (Ravnik et al. PRL 07)

STRETCHING OF DIMERS

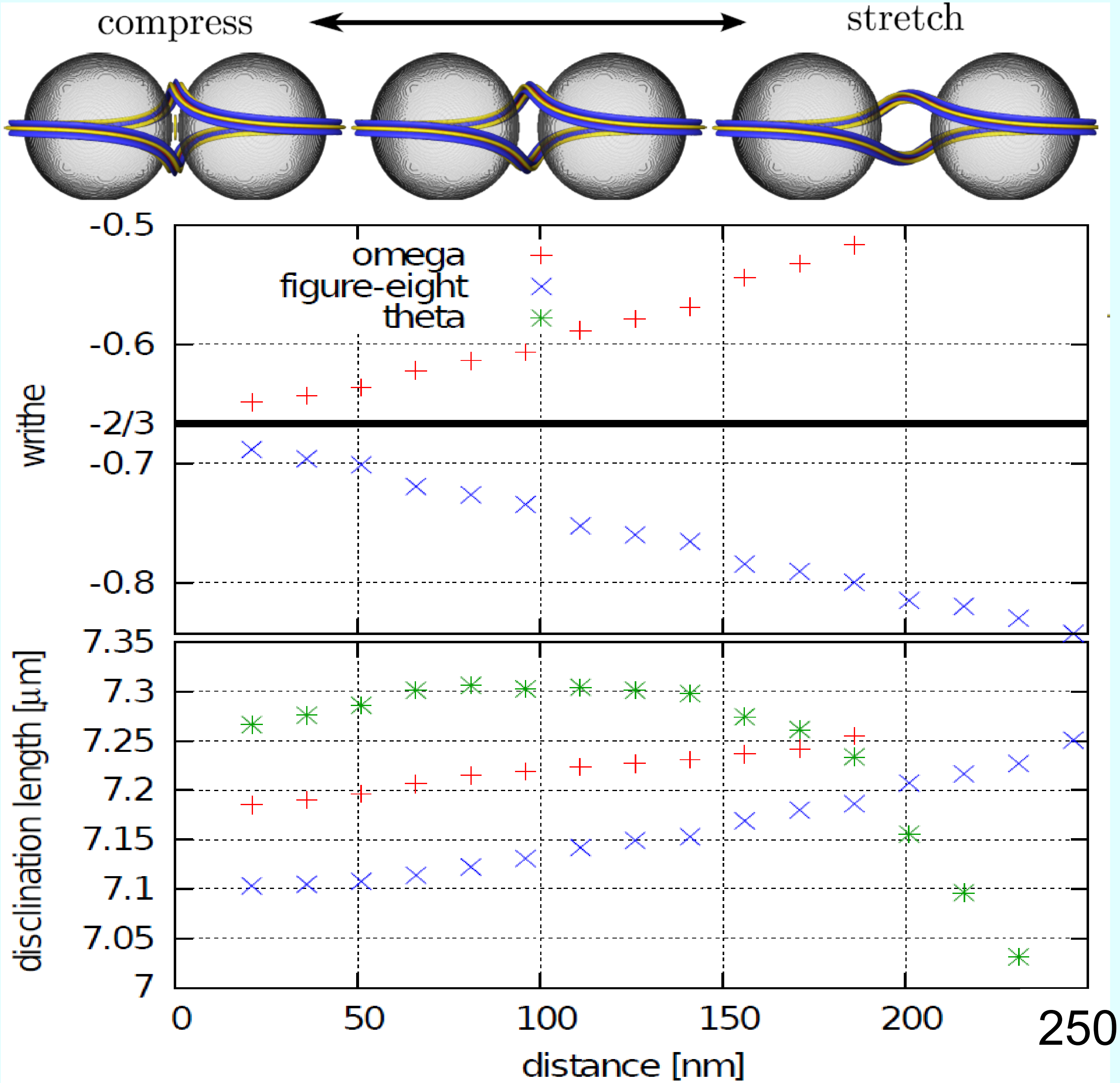

Cell thickness 1.5 µm
Diameter 1 µm

Copar, Porenta, and Zumer PRE 2011

DIMER IN TWISTED NEMATIC FIELD

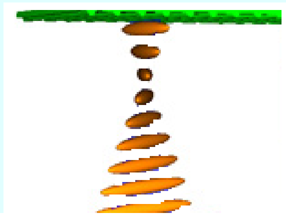

Cell thickness 1.5 μm, particle diameter 1 μm

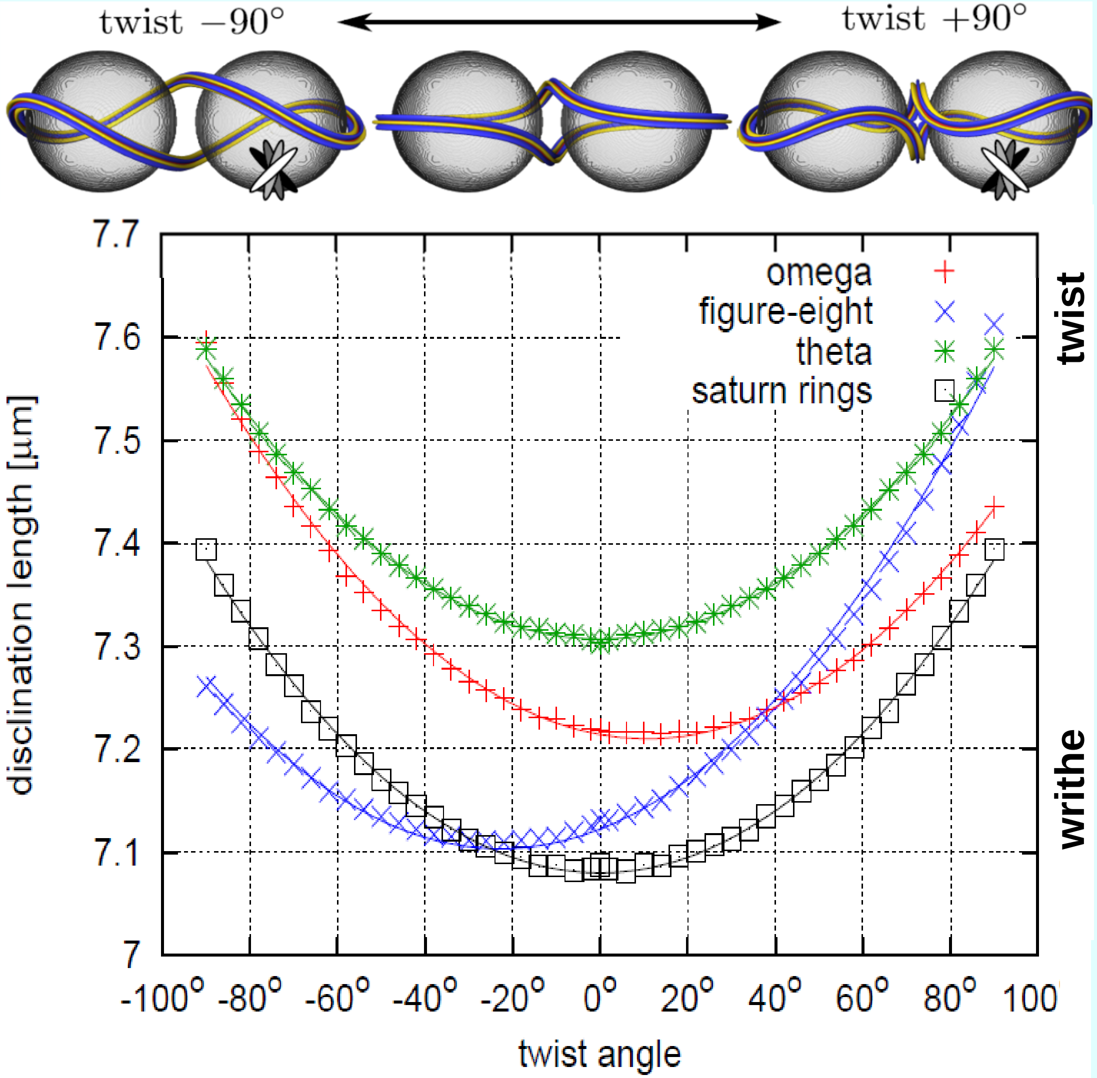

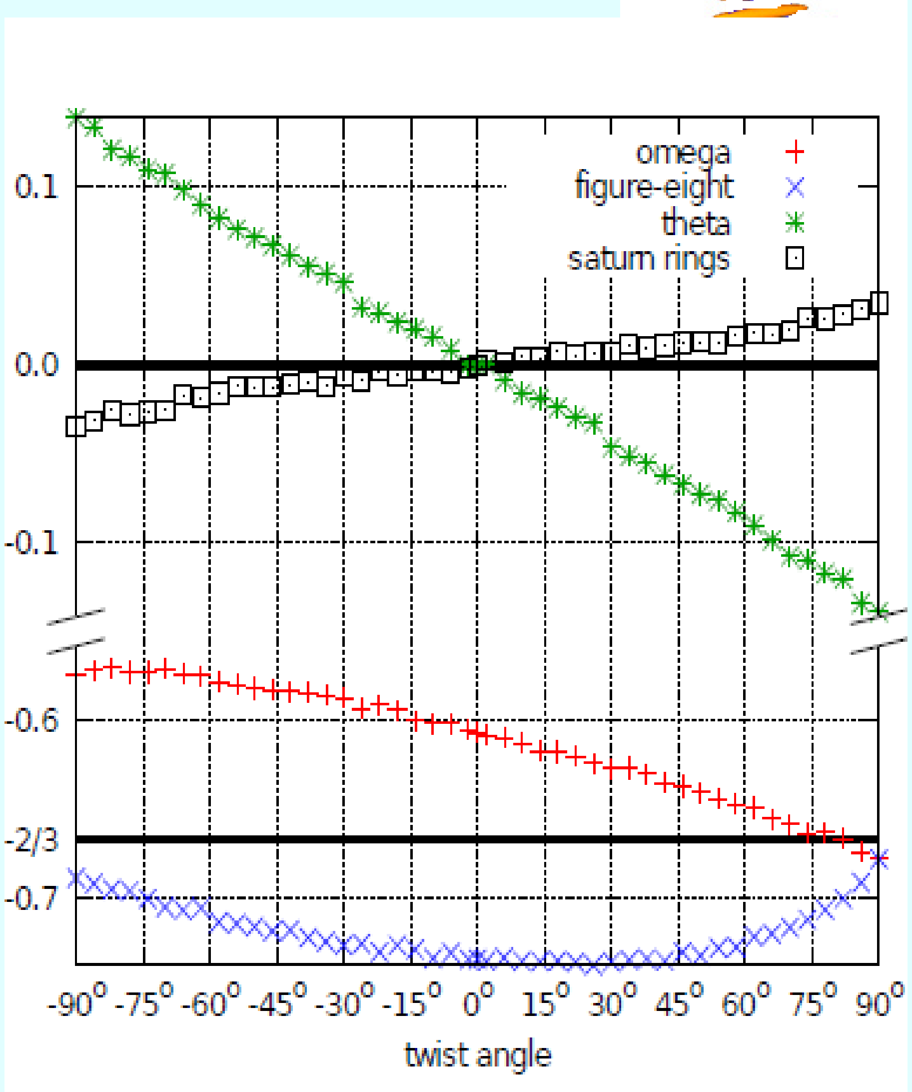

Copar, Porenta, and Zumer PRE 2011

ADDITIONAL REWIRING POSSIBILITIES IN TWISTED CELLS

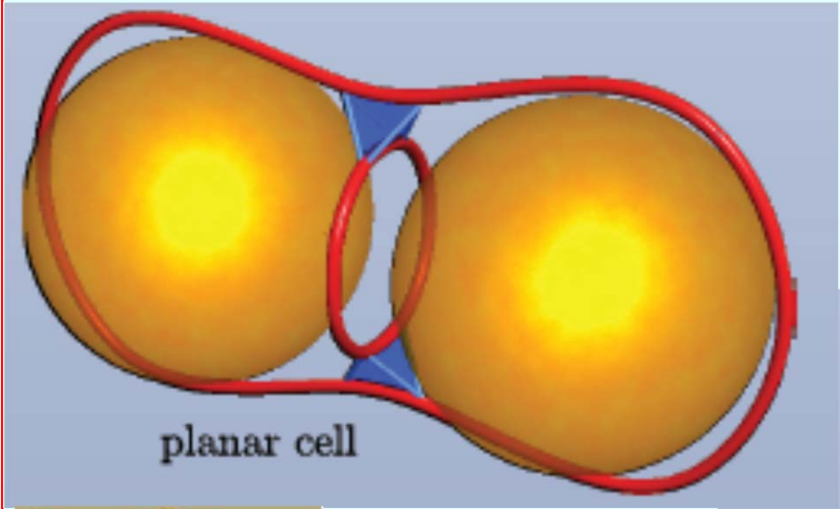

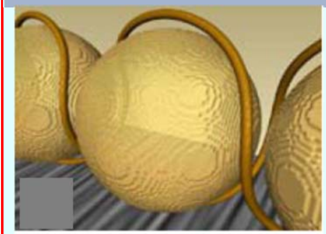

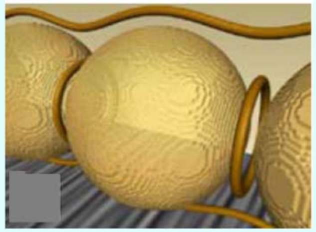

6 different dimer structures

tetrahedral rewiring sites between four neighboring particles are possible leading to knots and links

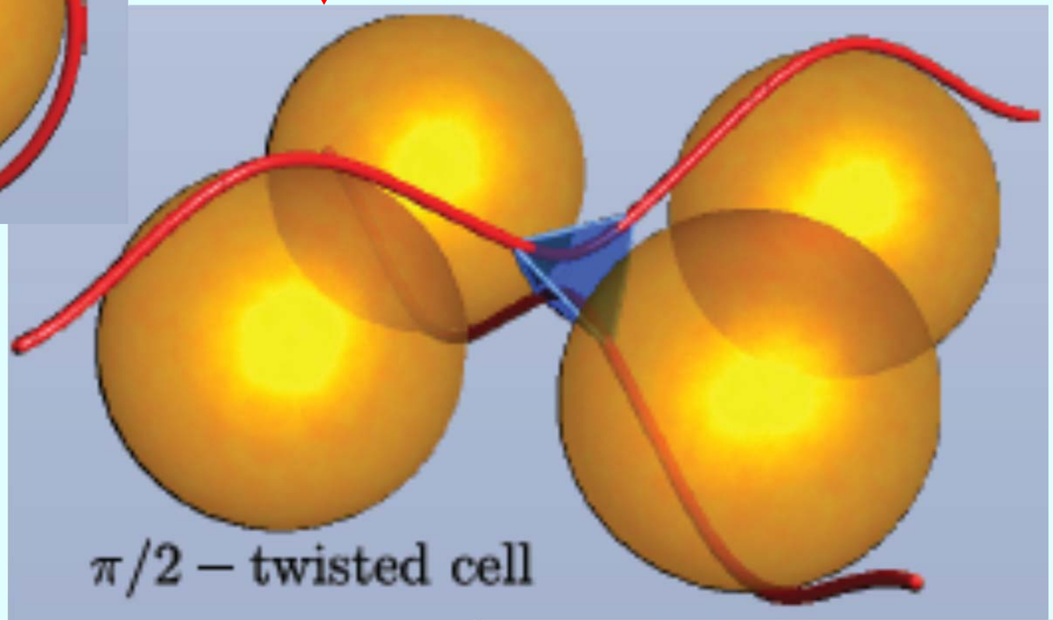

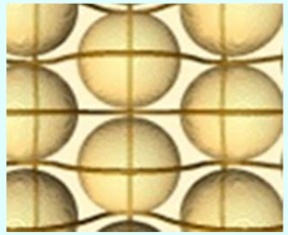

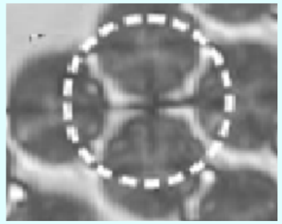

INCREASING TWIST

V.S.R. Jampani et al. PRE 2011

36 possible dimer structures are predicted. One is linked: Hopf link.

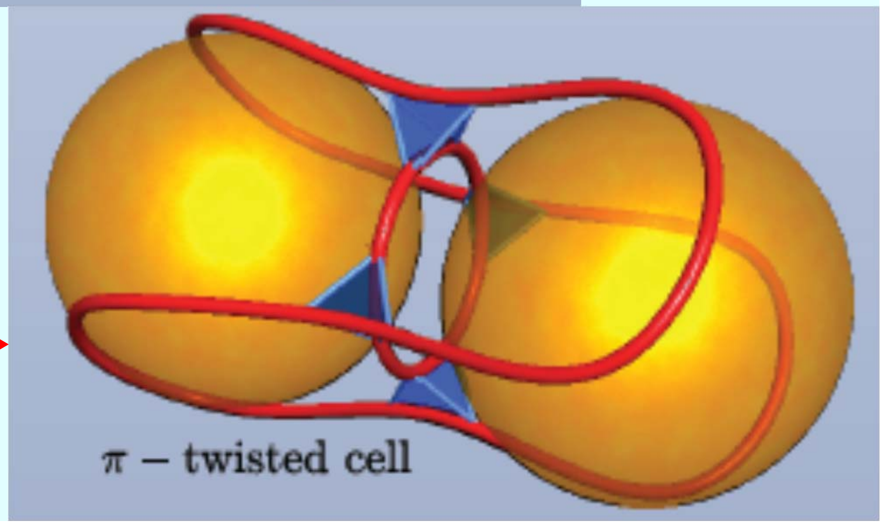

ENTANGLED DIMER IN A π-CELL

TWISTED NEMATIC yields here 4 rewiring sites (A,B,C,D) . right handed

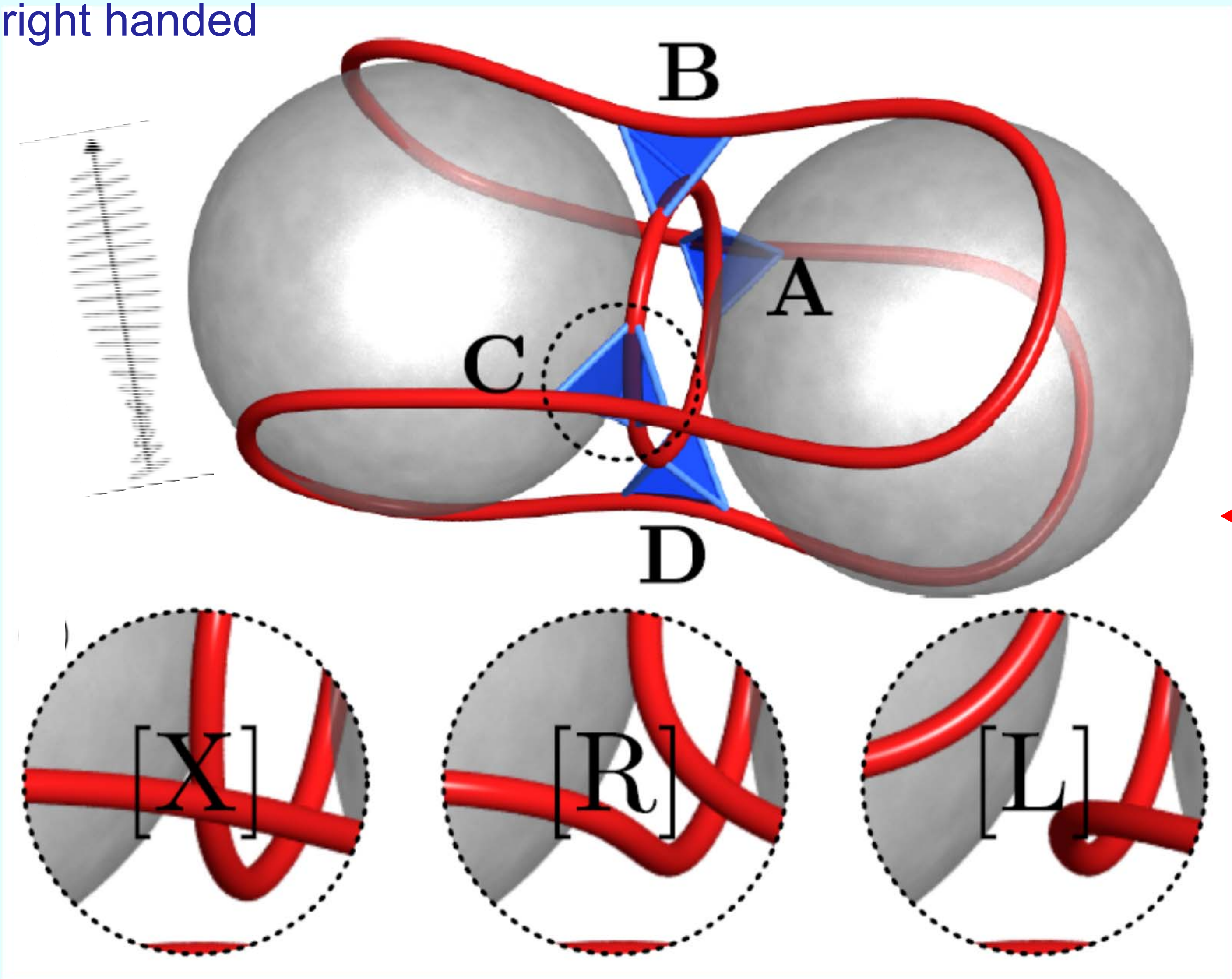

Each of them can assume states [X], [R], [L], producing 81 states, 36 of which are different. The structures are specified by their [ABCD] codes.

This structure has the code [XXXX].

How many are stable?

Copar et al. 2012

FROM ANSATZ TO A STABLE SOLUTION

Ansatz : cubic spline and spherical arcs in rewiring tetrahedrons

[XXRX] is stable

[XXLX] is unstable

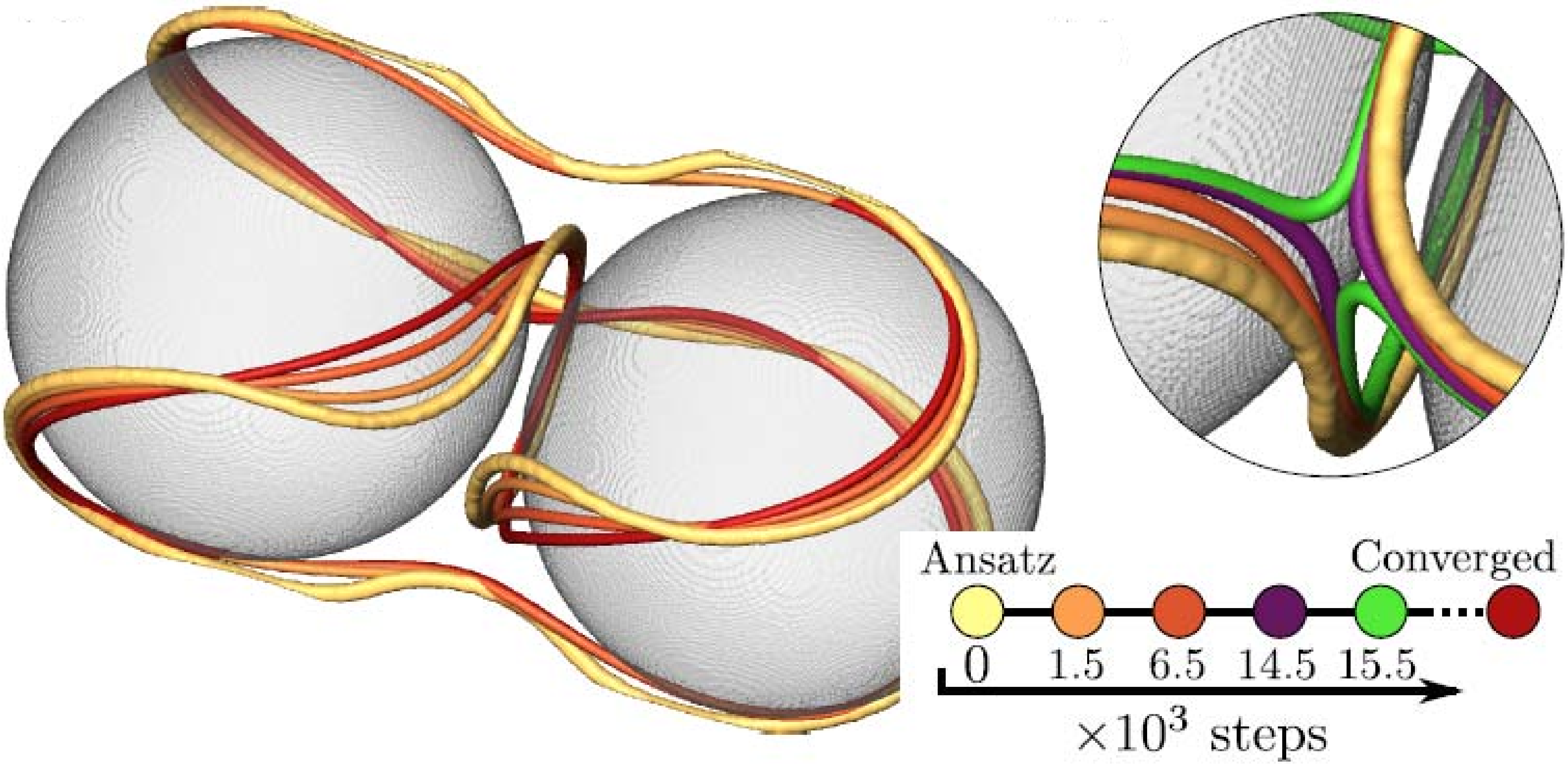

Copar et al. 2012

OBSERVED DIMER STRUCTURES:
STABLE & METASTABLE

Simulations & experiment :

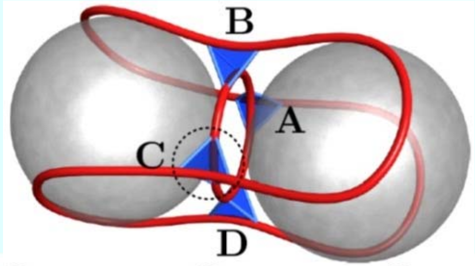

Only experimentally:

2 twisted Saturn rings

Hopf link

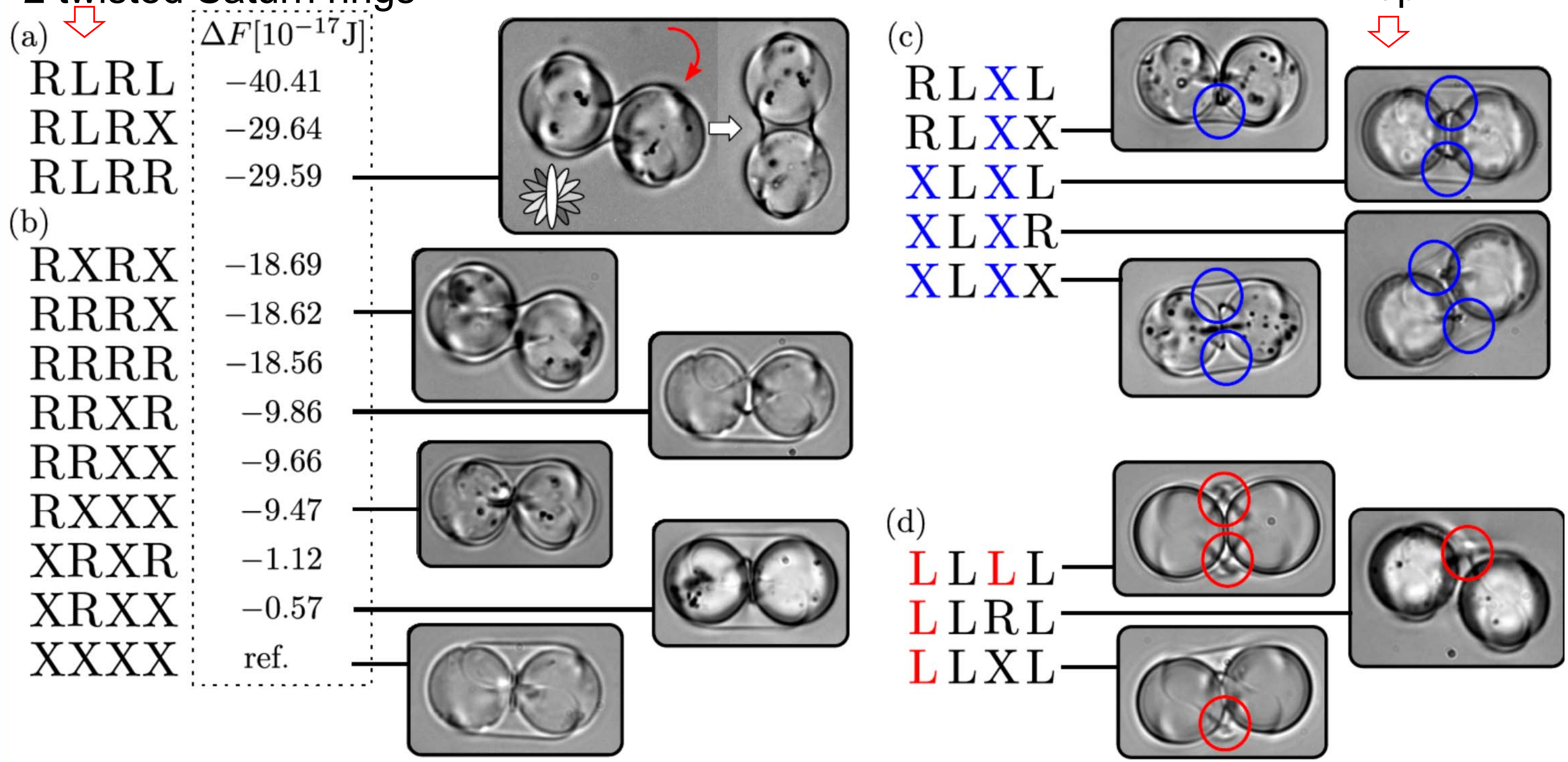

[L] tangles at A & C sites are the most expenseve.

Copar et al. 2012

EVOLUTION OF TANGLES IN SIMULATION TIME

RIGHT π TWISTED NEMATIC CELL: C site

Stability of a tangle depends on other three tangles and sense of the twist in the cell. Local large twist deviations are shown by green isosurfaces.

Stable [R] tangle

Stable [X] tangle

Unstable [X] & [R] tangles exhibit a formation of the bridge of increased twist deviation and splay-bend parameter, followed by the rewiring of the disclinations.

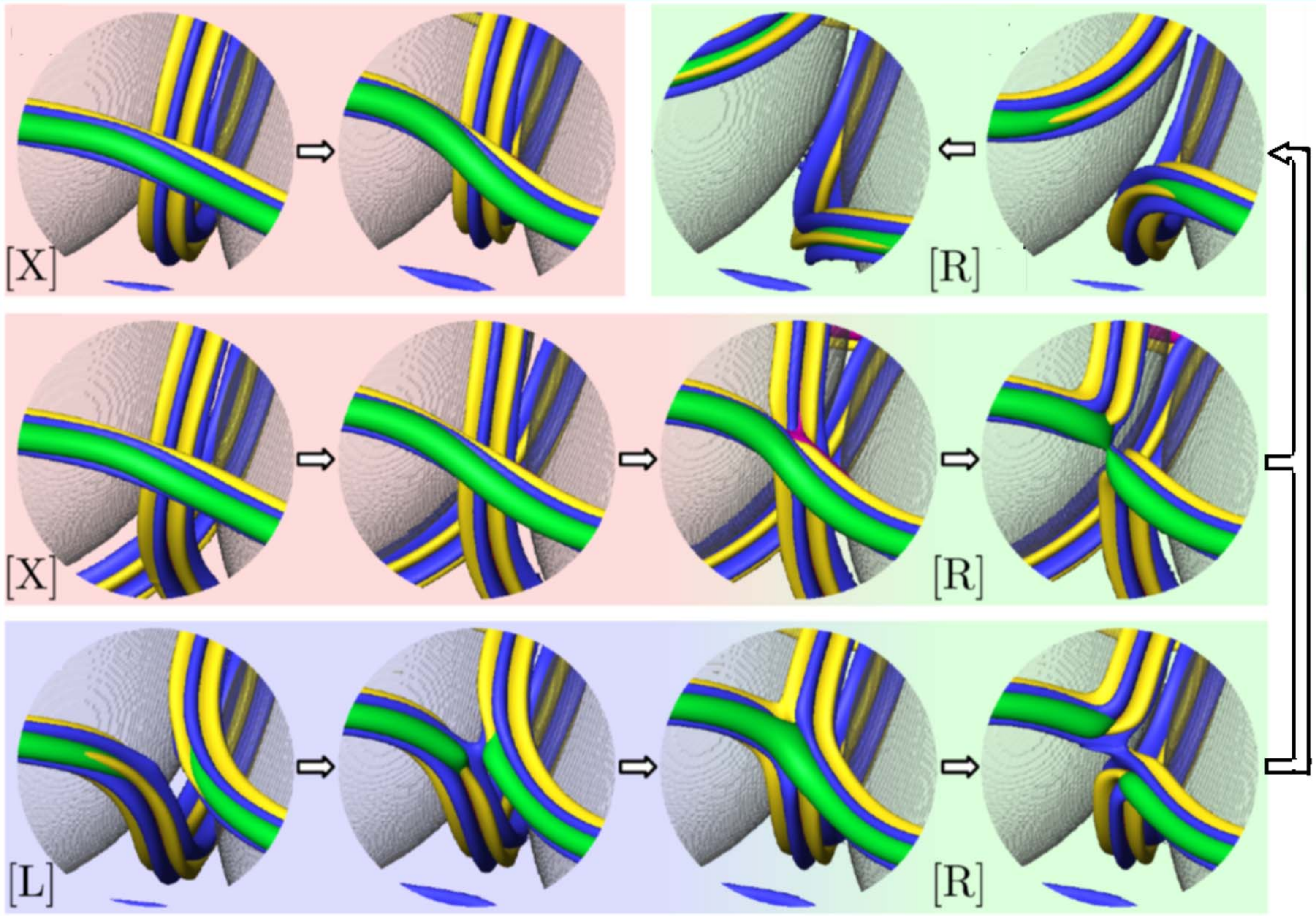

Copar et al. 2012

KNOTS LINKS IN TN CELL
OPTICAL TWEEZERS ASSISTED ASSEMBLY

Experiments: ~4.7μm homeotropic silica particles in ~ 6μm thick left handed 90° TN cell.

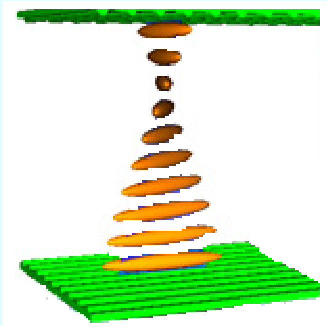

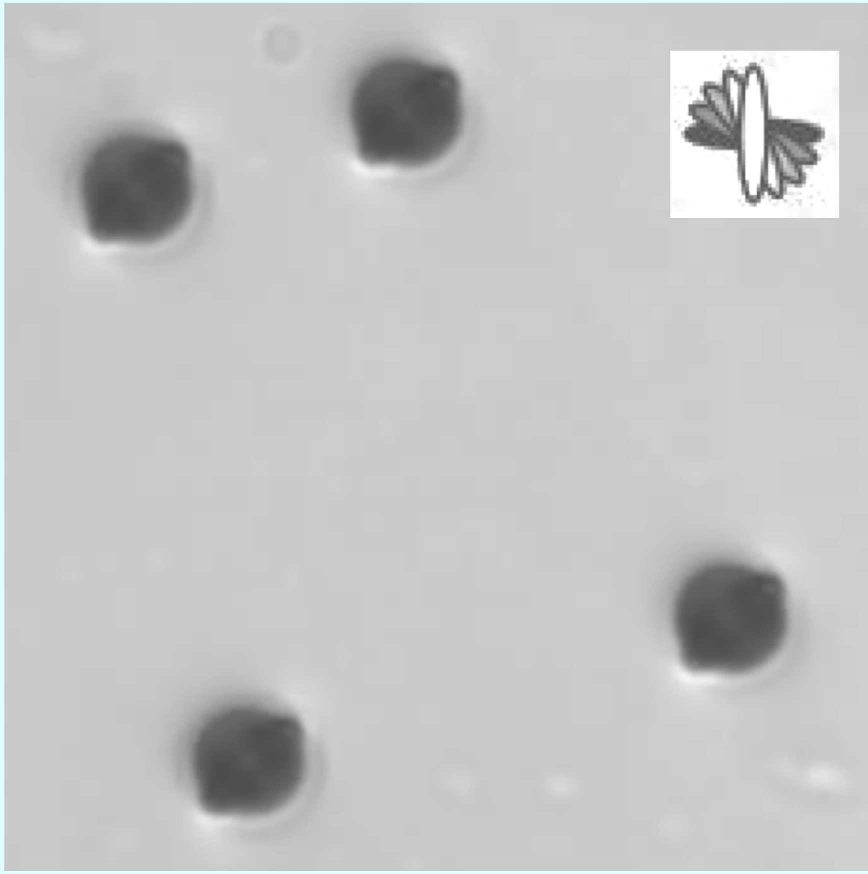

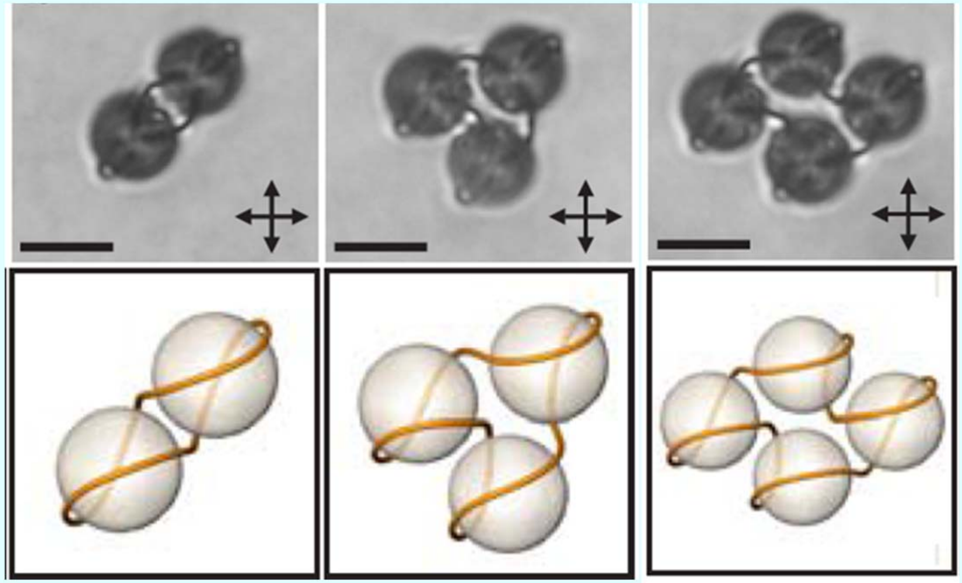

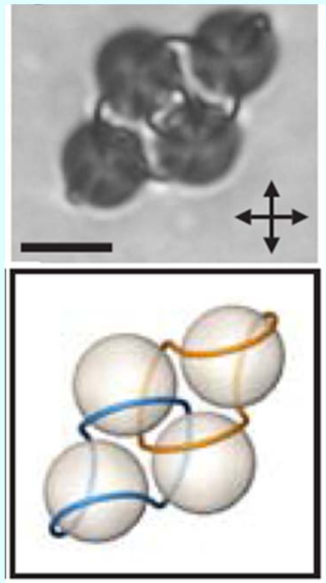

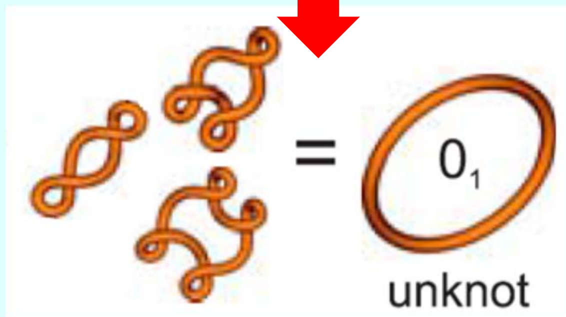

Tkalec, Ravnik, Copar, Zumer, Musevic; Science 2011

FORMING KNOTS : TREFOIL

4.7μm homeotropic silica particles in 6μm thick left handed 90° TN cell.

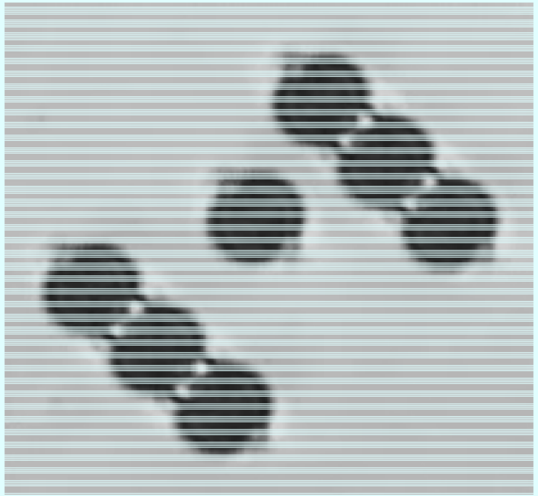

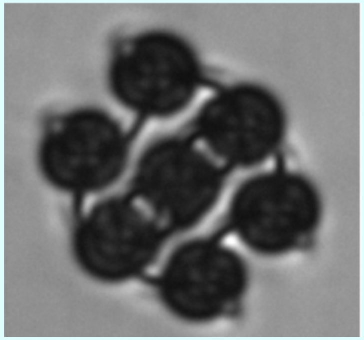

Complex conformation of the disclination loop is equivalent to the trefoil knot:

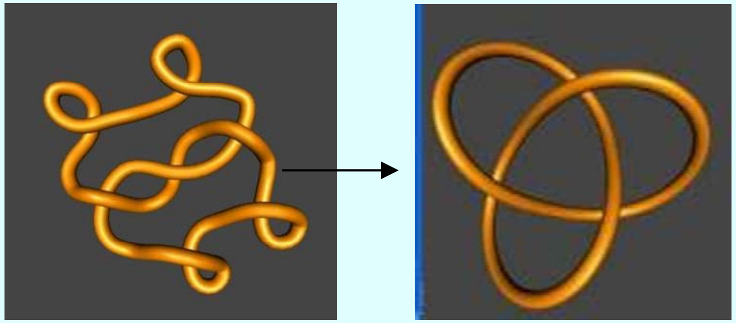

Continuous transformation of the disclination loop (Raidemeister moves):

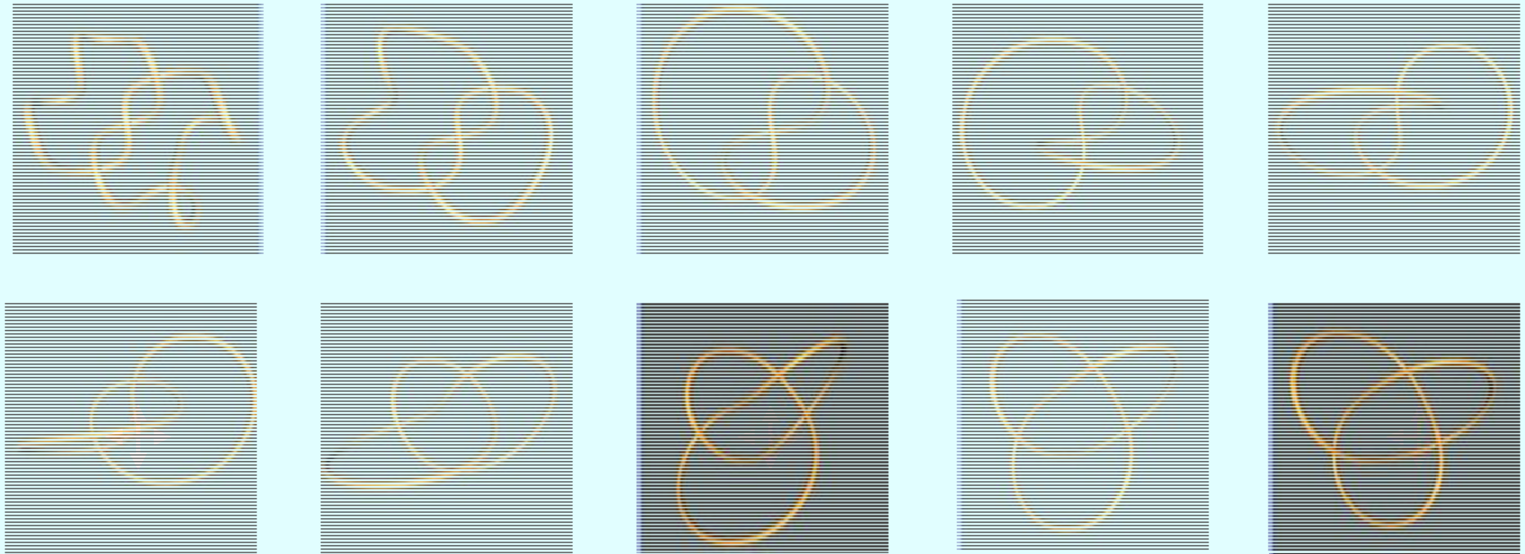

Tkalec et al. Science 2011

KNOTS AND LINKS – RECONFIGURABILITY

Reconfiguration by changing local tangles:

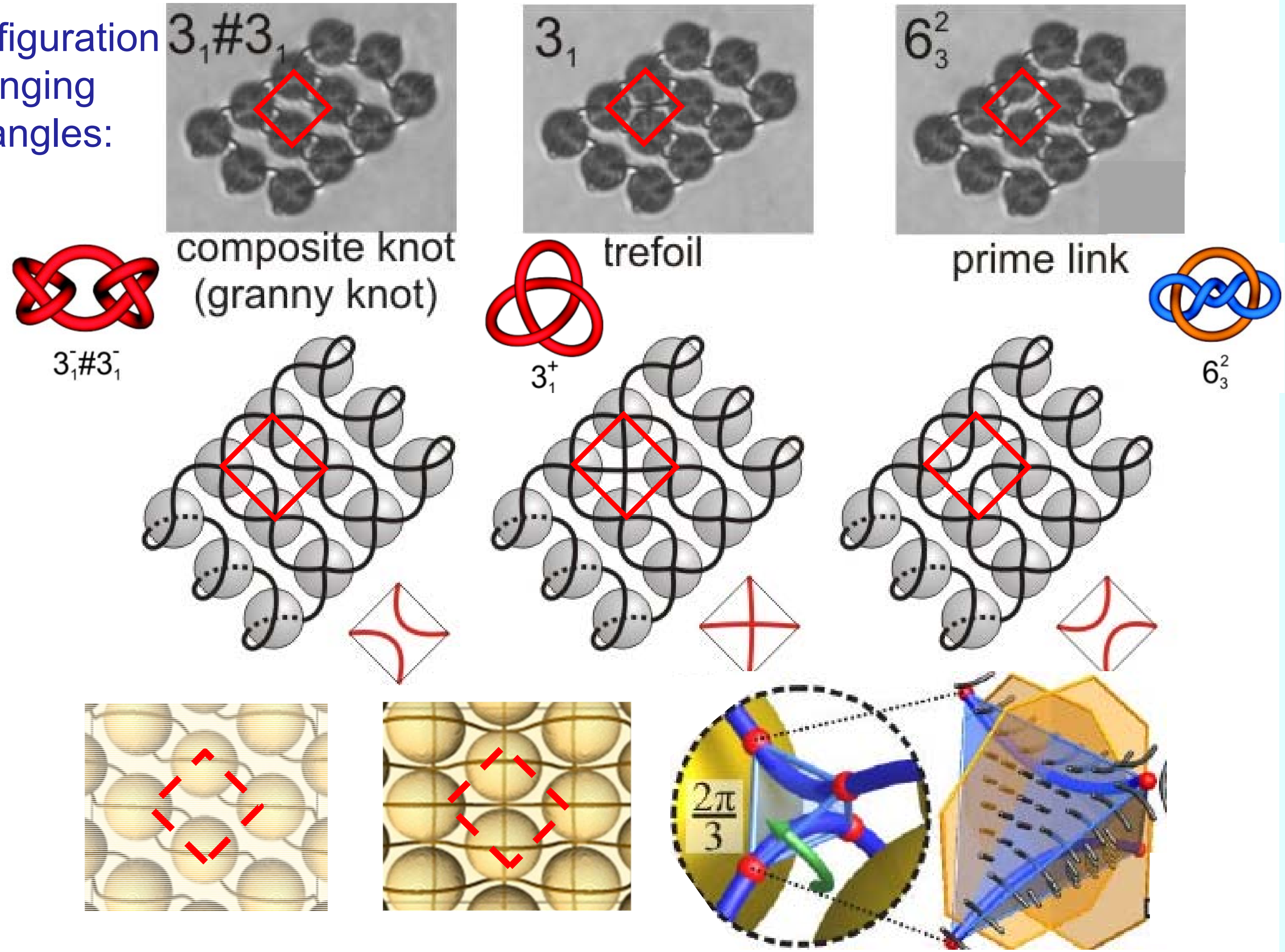

Tkalec et al. Science 2011

CLASIFICATION OF ENTANGLED DISCLINATION LOOPS

Topological invariant Sl - self-linking number - is here used to classify entangled disclination loops in addition to standard quantities C - number of crossings - and N - number od loops -.

Some of the observed loops.

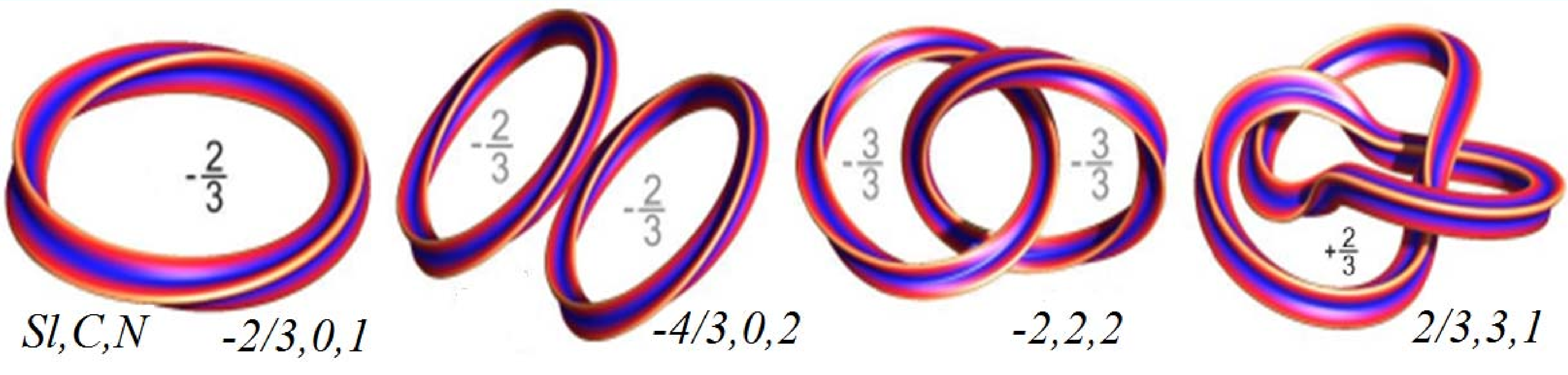

Tkalec et al. Science 2011

Copar & Zumer, PRL 2011

CLASSIFICATION OF KNOTS AND LINKS:
SELF-LINKING NUMBER AND NUMBER OF LOOPS

Array of tangles (*p* x *q* particles):

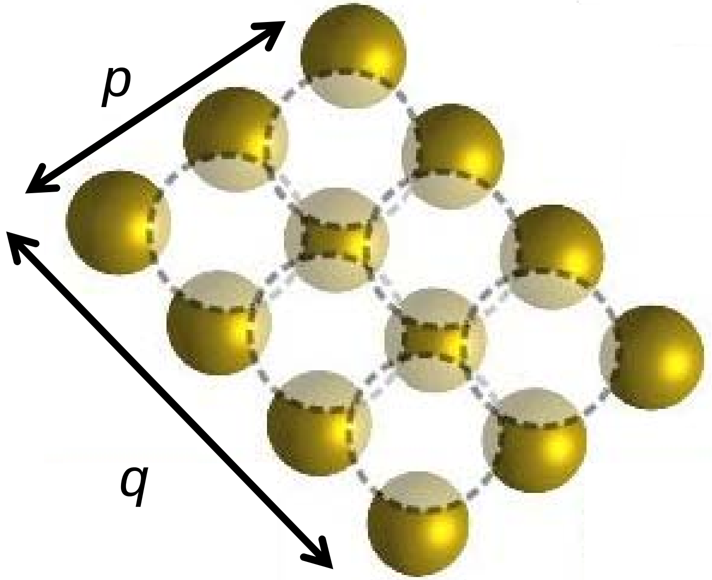

p x *q* particles

⇩

(*p* - 1) x (*q* - 1) tangles

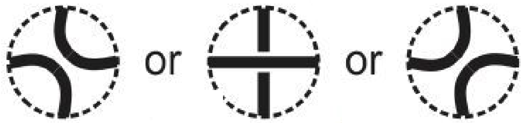

⇩

$3^{(p-1)(q-1)}$ tangle combinations

Classification of all states (knots and links):

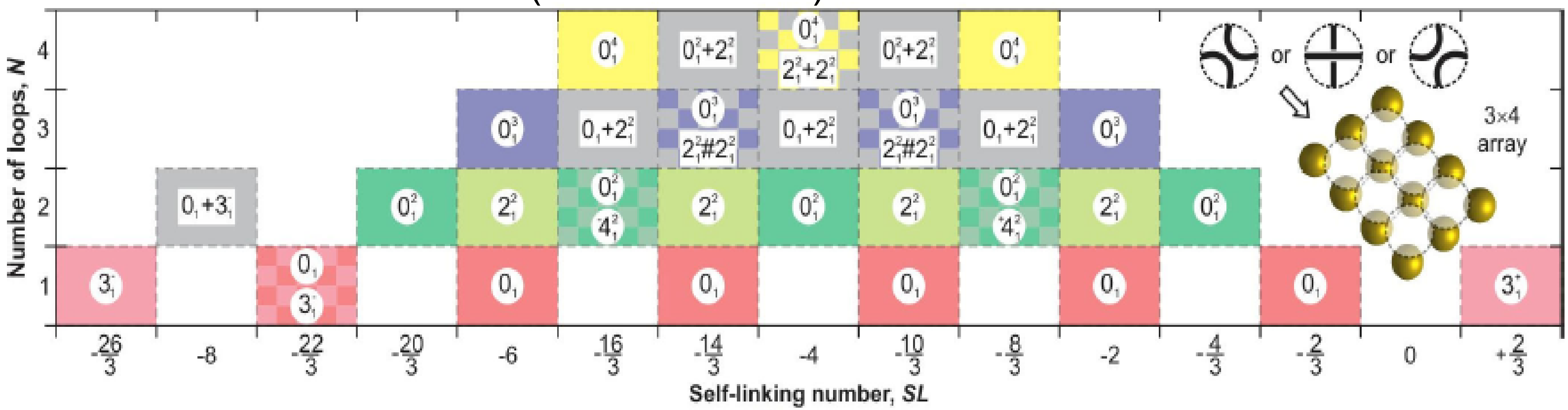

Tkalec et al. Science 2011

ASSEMBLY OF KNOTS AND LINKS: 4 x 4 CASE

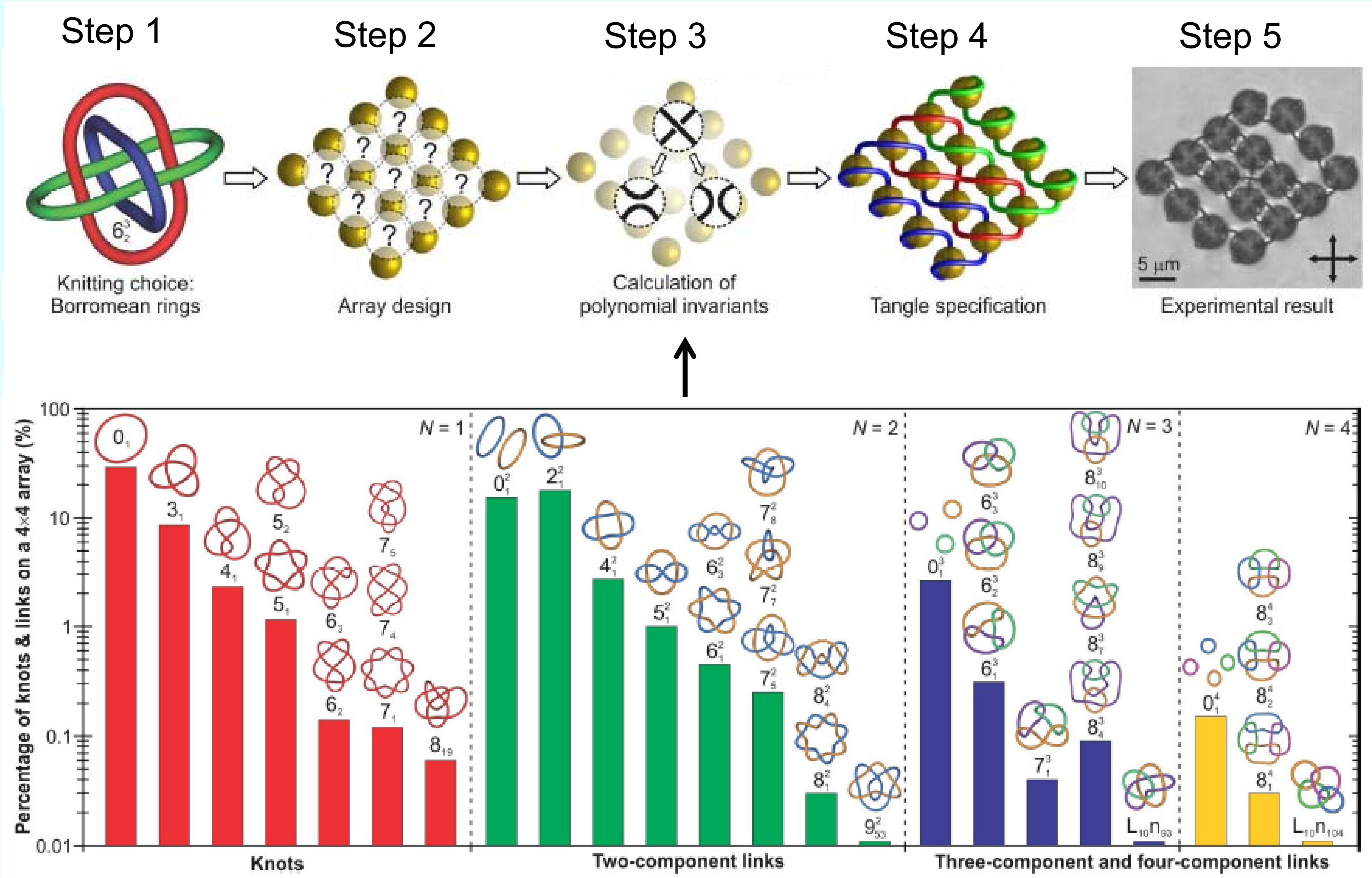

Tkalec et al. Science 2011

PERSPECTIVES: MORE HIGHLY TWISTED CASES

top – bottom right twist of the director field in a TN cell with a colloid; Top views:

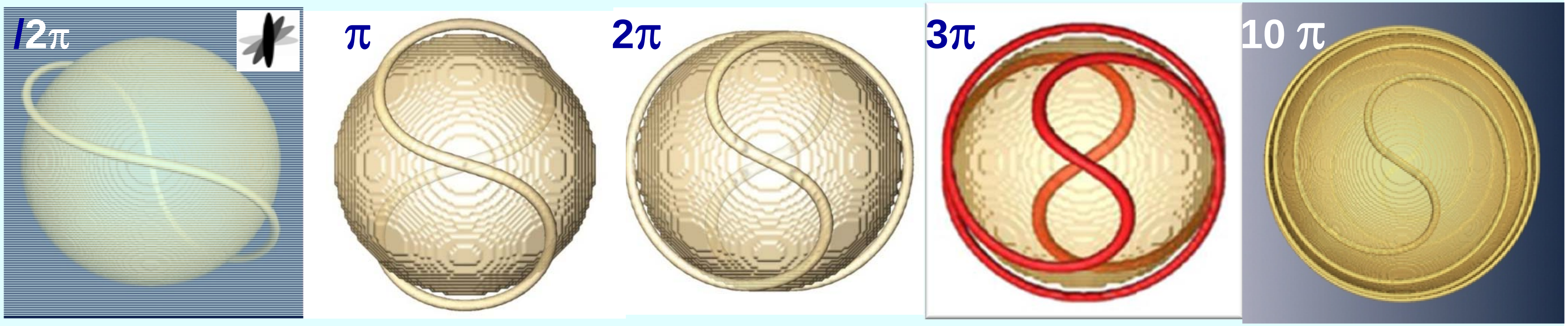

Marenduzzo et al. 2010, Ravnik 2008 & 2010

3D structure

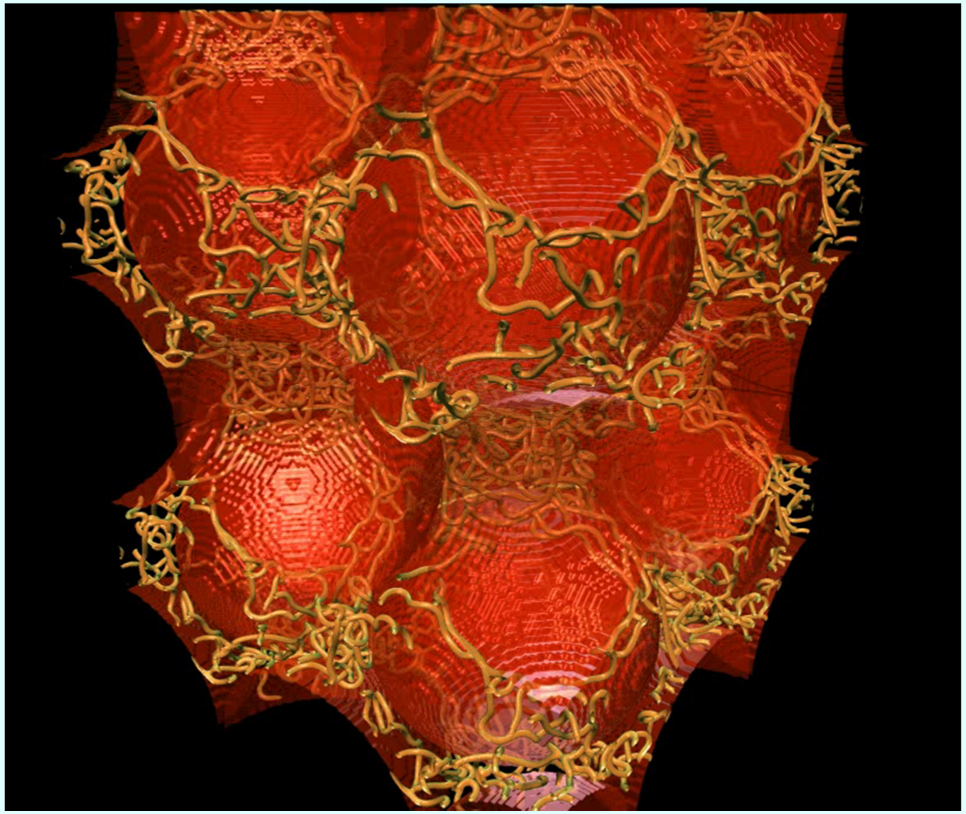

Copar 2011

CONCLUSIONS

- Sharing of deformation field and disclinations are the crucial mechanisms for nematic mediated interaction in micron size colloids.
- Topological description of nematics braids that entangle colloidal particles a new topological invariant of a disclination loop - self-linking number - is introduced.
- In nematic braids with orthogonal crossing of disclinations a tetrahedron restructuring was introduced.
- Restructuring from an ansatz to a stable structure during the numerical simulation
- Knots and links and their reconfiguration in chiral nematic colloids is classified within the standard knot theory complemented by our topology of nematic loops.
- Further steps: highly twisted systems from colloids to blue phases

The above discussed examples of topological soft matter are expected to have potential beyond a topological playground.